J|A|C|S
ARTICLES
Published on Web 06/23/2006

On the Mechanism of the Copper-Catalyzed Enantioselective 1,4-Addition of Grignard Reagents to α,β-Unsaturated Carbonyl Compounds

Syuzanna R. Harutyunyan, Fernando López,† Wesley R. Browne, Arkaitz Correa, Diego Peña,† Ramon Badorrey,‡ Auke Meetsma, Adriaan J. Minnaard,* and Ben L. Feringa*

Contribution from the Department of Organic Chemistry and Molecular Inorganic Chemistry, Stratingh Institute, University of Groningen, Nijenborgh 4, 9747 AG Groningen, The Netherlands

Received December 18, 2005; E-mail: B.L.Feringa@rug.nl

Abstract: The mechanism of the enantioselective 1,4-addition of Grignard reagents to α,β-unsaturated carbonyl compounds promoted by copper complexes of chiral ferrocenyl diphosphines is explored through kinetic, spectroscopic, and electrochemical analysis. On the basis of these studies, a structure of the active catalyst is proposed. The roles of the solvent, copper halide, and the Grignard reagent have been examined. Kinetic studies support a reductive elimination as the rate-limiting step in which the chiral catalyst, the substrate, and the Grignard reagent are involved. The thermodynamic activation parameters were determined from the temperature dependence of the reaction rate. The putative active species and the catalytic cycle of the reaction are discussed.

Introduction

The copper-catalyzed conjugate addition (CA) of organometallic reagents to α,β-unsaturated carbonyl compounds is one of the most versatile synthetic methods for the construction of C−C bonds.[1] Catalytic enantioselective versions of this transformation employing chiral copper complexes[2−5] have been achieved primarily with organozinc reagents,[2−4a,b] although organoaluminum compounds have proven to be successful also.[4c−e] The inherently low reactivity of organozinc reagents toward unsaturated carbonyl compounds has facilitated the development of a plethora of chiral phosphorus-based ligands (i.e. phosphoramidites, phosphines, phosphonites) capable of providing highly efficient ligand-accelerated catalysis with excellent enantioselectivities over a broad range of substrates.[2,3]

In contrast, the application of Grignard reagents, which are among the most widely used of organometallic compounds, in the CA to α,β-unsaturated carbonyl systems has received much less attention.[6] Despite intensive research over the last two decades, only modest selectivity in the CA of Grignard reagents was observed in comparison to dialkyzinc reagents.[6] This is most probably due to the higher reactivity of Grignard reagents, which

† Present address: Departamento de Química Orgánica, Facultad de Química, Universidad de Santiago de Compostela, 15706 Santiago de Compostela, Spain.

‡ Present address: Departamento de Química Orgánica, Facultad de Ciencias, Instituto de Ciencia de Materiales de Aragón, Universidad de Zaragoza, Consejo Superior de Investigaciones Científicas, 50009 Zaragoza, Spain.

(1) (a) Perlmutter, P. *Conjugate Addition Reactions in Organic Synthesis*; Tetrahedron Organic Chemistry, Series 9; Pergamon: Oxford, 1992. (b) Rossiter, B. E.; Swingle, N. M. *Chem. Rev.* **1992**, *92*, 771−806..

(2) (a) Feringa, B. L.; de Vries, A. H. M. In *Asymmetric Chemical Transformations*; Doyle, M. D., Ed.; Advances in Catalytic Processes; JAI Press Inc.: Greenwich, 1995; Vol. 1, pp 151−192. (b) Krause, N. *Angew. Chem., Int. Ed.* **1998**, *37*, 283−285. (c) Tomioka, K.; Nagaoka, Y. In *Comprehensive Asymmetric Catalysis*; Jacobsen, E. N., Pfaltz, A., Yamamoto, H., Eds.; Springer-Verlag: New York, 1999; Vol. 3, pp 1105−1120. (d) Sibi, M. P.; Manyem, S. *Tetrahedron* **2000**, *56*, 8033−8061. (e) Krause, N.; Hoffmann-Röder, A. *Synthesis* **2001**, 171−196.

(3) (a) Feringa, B. L.; Naasz, R.; Imbos, R.; Arnold, L. A. In *Modern Organocopper Chemistry*; Krause, N., Ed.; Wiley-VCH: Weinheim, Germany, 2002; pp 224−258. (b) de Vries, A. H. M.; Meetsma, A.; Feringa, B. L. *Angew. Chem., Int. Ed. Engl.* **1996**, *35*, 2374−2376. (c) Feringa, B. L.; Pineschi, M.; Arnold, L. A.; Imbos, R.; de Vries, A. H. M. *Angew. Chem., Int. Ed. Engl.* **1997**, *36*, 2620−2623.

(4) (a) Mizutani, H.; Degrado, S. J.; Hoveyda, A. H. *J. Am. Chem. Soc.* **2002**, *124*, 779−781. (b) Alexakis, A.; Benhaim, C. *Eur. J. Org. Chem.* **2002**, 3221−3236 and references therein. (c) For an addition of $AlMe_3$ to linear aliphatic enones, see: Frase, P. K.; Woodward, S. *Chem.—Eur. J.* **2003**, *9*, 776−783. (d) Hayashi, T.; Ueyama, K.; Tokunaga, N.; Yoshida, K. *J. Am. Chem. Soc.* **2003**, *125*, 11508−11509. (e) Alexakis, A.; Albrow, V.; Biswas, K.; d'Augustin, M.; Prieto, O.; Woodward, S. *Chem. Commun.* **2005**, *22*, 2843−2845.

(5) For recent advances in the catalytic enantioselective conjugate reduction of α,β-unsaturated carbonyl compounds, which provides an alternative route to the optically active β-substituted carbonyl compounds see: (a) Lipshutz, B. H.; Servesko, J. M. *Angew. Chem., Int. Ed.* **2003**, *42*, 4789−4792. (b) Lipshutz B. H.; Servesko, J. M.; Taft, B. R. *J. Am. Chem. Soc.* **2004**, *126*, 8352−8353. (c) Lipshutz, B. H.; Frieman, B. A. *Angew. Chem., Int. Ed.* **2005**, *44*, 6345−6348.

(6) (a) Villacorta, G. M.; Rao, C. P.; Lippard, S. J. *J. Am. Chem. Soc.* **1988**, *110*, 3175−3182. (b) Ahn, K.-H.; Klassen, R. B.; Lippard, S. J. *Organometallics* **1990**, *9*, 3178−3181. (c) Lambert, F.; Knotter, D. M.; Janssen, M. D.; van Klaveren, M.; Boersma, J.; van Koten, G. *Tetrahedron: Asymmetry* **1991**, *2*, 1097−1100. (d) Knotter, D. M.; Grove, D. M.; Smeets, W. J. J.; Spek, A. L.; van Koten, G. *J. Am. Chem. Soc.* **1992**, *114*, 3400−3410. (e) Spescha, D.; Rihs, G. *Helv. Chim. Acta* **1993**, *76*, 1219−1230. (f) Zhou, Q.-L.; Pfaltz, A. *Tetrahedron* **1994**, *50*, 4467−4478. (g) Braga, A. L.; Silva, S. J. N.; Lüdtke, D. S.; Drekener, R. L.; Silveira, C. C.; Rocha, J. B. T.; Wessjohann, L. A. *Tetrahedron Lett.* **2002**, *43*, 7329−7331. (h) Seebach, D.; Jaeschke, G.; Pichota, A.; Audergon, L. *Helv. Chim. Acta* **1997**, *80*, 2515−2519. (i) Pichota, A.; Pregosin, P. S.; Valentini, M.; Wörle, M.; Seebach, D. *Angew. Chem., Int. Ed.* **2000**, *39*, 153−156. (j) Kanai, M.; Tomioka, K. *Tetrahedron Lett.* **1995**, *36*, 4275−4278. (k) Nakagawa, Y.; Kanai, M.; Nagaoka, Y.; Tomioka, K. *Tetrahedron* **1998**, *54*, 10295−10307. (l) Kanai, M.; Nakagawa, Y.; Tomioka, K. *Tetrahedron* **1999**, *55*, 3843−3854. (m) Stangeland, E. L.; Sammakia, T. *Tetrahedron* **1997**, *53*, 16503−16510.

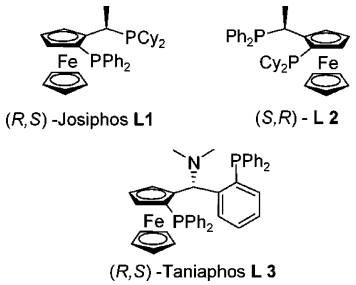

Figure 1. Chiral ligands used in the CA of Grignard reagents.

Scheme 1. Enantioselective CA of Grignard Reagents to α,β-Unsaturated Compounds

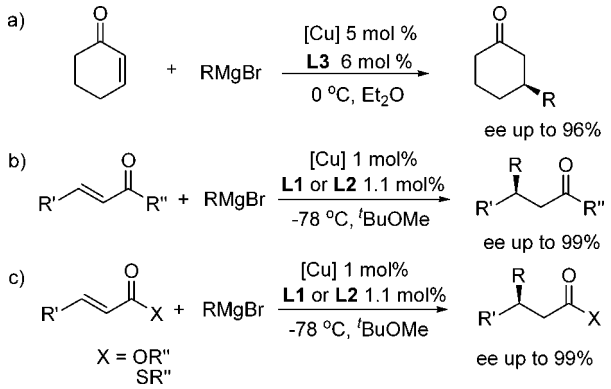

leads to uncatalyzed 1,2- and 1,4-additions. Moreover, the presence of several competing organometallic complexes in solution (typical of cuprate chemistry) further complicates access to effective enantioselective catalysis.

Recently, we demonstrated that high enantioselectivities (up to 99% ee) can be achieved in the CA of Grignard reagents to α,β-unsaturated carbonyl compounds using catalytic amounts of chiral ferrocenyl diphosphine ligands and Cu(I) salts (Figure 1, Scheme 1).[7] Most notably, the Josiphos- and Taniaphos-type ligands (Figure 1) allow for a broad substrate scope to be used successfully in these reactions, including cyclic and acyclic enones, enoates, and thioenoates (Scheme 1). Despite these breakthroughs, the nature of the complexes involved and a rationalization of the electronic factors, which govern the substrate specificity of the various Cu(I)−ferrocenyl-diphosphine complexes is highly desirable. A detailed understanding of the reaction mechanism, including the generation of the active species, insight into key steps in the catalytic cycle, and kinetic information is essential for the elucidation of the mechanism and future rational improvement of this important transformation.

The mechanism of the copper-catalyzed enantioselective CA of organometallic compounds may follow similar principles as proposed for the noncatalytic organocuprate addition.[8,9] A

Scheme 2. Proposed Mechanistic Pathway for the Stoichiometric 1,4-Addition of Organocuprates

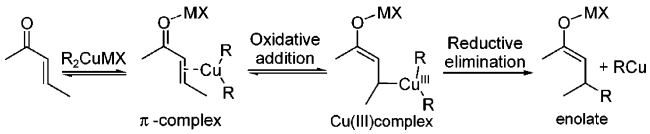

widely accepted mechanism (Scheme 2) for noncatalytic organocuprate addition is supported by kinetic studies,[9a,b] in particular kinetic isotope effect measurements[9c,d] and NMR spectroscopy[9e,f] of intermediates observed during the reaction. The current mechanistic view is that the CA of organometallic compounds proceeds through reversible formation of a copper−olefin π-complex, involving d,π* back-donation,[9e−h] followed by a formal oxidative addition to the β-carbon leading to a d^8 copper(III) intermediate[9h−k] and, finally, reductive elimination to form the enolate (Scheme 2).

Although π-complexes for α, β-unsaturated esters, ketones, and nitriles have been observed by low-temperature NMR spectroscopy,[10] direct observation of copper(III) intermediates has not been achieved in organocuprate CA, and their involvement is supported primarily through quantum-chemical calculations.[11] Experimental and theoretical studies made by Snyder et al.[9c] and Krause et al.[9d] on organocuprate CAs indicate that the rate-determining step is the C−C bond formation via reductive elimination of the copper(III) intermediate (Scheme 2).

On the basis of the cumulative mechanistic data obtained for the stoichiometric organocuprate CA, a similar mechanism for the copper-catalyzed enantioselective CA of dialkylzinc reagents, involving an oxidative addition−reductive elimination pathway, has been postulated.[12] However, relatively few mechanistic studies have been reported to date for the enantioselective copper-catalyzed CA of any class of organometallic reagent.[13] Moreover, these studies are related, exclusively, to the catalytic CA of dialkylzinc reagents and have not, as yet, led to a general

(7) (a) Feringa, B. L.; Badorrey, R.; Peña, D.; Harutyunyan, S. R.; Minnaard, A. J. *Proc. Natl. Acad. Sci. U.S.A.* **2004**, *101*, 5834−5838. (b) López, F.; Harutyunyan, S. R.; Minnaard, A. J.; Feringa, B. L. *J. Am. Chem. Soc.* **2004**, *126*, 12784−12785. (c) López, F.; Harutyunyan, S. R.; Minnaard, A. J.; Feringa, B. L. *Angew. Chem., Int. Ed.* **2005**, *44*, 2752−2756. (d) Des Mazery, R.; Pullez, M.; López, F.; Harutyunyan, S. R.; Minnaard, A. J.; Feringa, B. L. *J. Am. Chem. Soc.* **2005**, *127*, 9966−9967. (e) Woodward, S. *Angew. Chem., Int. Ed.* **2005**, *44*, 5560−5562.

(8) For reviews on reaction mechanisms of organocuprates, see: (a) Woodward, S. *Chem. Soc. Rev.* **2000**, *29*, 393−401 and references therein. (b) Nakamura E.; Mori S. *Angew. Chem., Int. Ed.* **2000**, *39*, 3750−3771. (c) Krause, N.; Gerold, A. *Angew. Chem., Int. Ed. Engl.* **1997**, *36*, 186−204. (d) Mori, S.; Nakamura, E. In *Modern Organocopper Chemistry*; Krause, N., Ed.; Wiley-VCH: Weinheim, Germany, 2002; pp 315−346.

(9) For mechanistic studies in organocuprates chemistry, see: (a) Krauss, S. R.; Smith, S. G. *J. Am. Chem. Soc.* **1981**, *103*, 141−148. (b) Canisius, J.; Gerold, A.; Krause, N. *Angew. Chem., Int. Ed.* **1999**, *38*, 1644−1645. (c) Frantz, D. E.; Singleton, D. A.; Snyder, J. P. *J. Am. Chem. Soc.* **1997**, *116*, 3383−3384. (d) Mori, S.; Uerdingen, M.; Krause, N.; Morokuma, K. *Angew. Chem., Int. Ed.* **2005**, *44*, 4715−4719. (e) Bertz, S. H.; Miao, G.; Eriksson, M. *Chem. Commun.* **1996**, 815−816. (f) Murphy, M. D.; Ogle, G.; Bertz, S. H. *Chem. Commun.* **2005**, 854−856. (g) Nilson, K.; Anderson, C.; Ullenius, A.; Gerold, A.; Krause, N. *Chem.—Eur. J.* **1998**, *4*, 2051−2058 and references therein. (h) Mori, S.; Nakamura, E. *Teterahedron Lett.* **1999**, *40*, 5319−5322. (i) Kingsbury, C. L.; Smith, R. A. *J. Am. Chem. Soc.* **1997**, *62*, 4629−4634. (j) Casey, C. P.; Cesa, M. *J. Am. Chem. Soc.* **1979**, *101*, 4236−4244. (k) Corey, E. J.; Boaz, N. *Tetrahedron Lett.* **1985**, *26*, 6015−6018. (l) Lipshutz, B. H.; Aue, D. H.; James, B. *Teterahedron Lett.* **1996**, *37*, 8471−8474.

(10) For low-temperature NMR studies in CAs of cuprates, see: (a) Christenson, B.; Olsson, T.; Ullenius, C. *Tetrahedron* **1989**, *45*, 523−534. (b) Bertz, S. H.; Smith, R. A. *J. Am. Chem. Soc.* **1989**, *111*, 8276−8277. (c) Bertz, S. H.; Carlin, M. K.; Deadwyler, D. A.; Murphy, M.; Ogle, C. A.; Seagle, P. H. A. *J. Am. Chem. Soc.* **2002**, *124*, 13650−13651. (d) Krause, N.; Wagner, R.; Gerold, A. *J. Am. Chem. Soc.* **1994**, *116*, 381−382 (e) Nilsson, K.; Ullenius, C.; Krause, N. *J. Am. Chem. Soc.* **1996**, *118*, 4194−4195. (f) Krause, N.; Wagner, R.; Gerold, A. *J. Am. Chem. Soc.* **1994**, *116*, 381−382. (g) See also refs 8 b, e−g.

(11) For the calculations that support the participation of Cu(III) intermediates in the CA of cuprates, see: (a) Nakamura, E.; Mori, S.; Morokuma, K. *J. Am. Chem. Soc.* **1997**, *119*, 4900−4910. (b) Yamanaka, M.; Nakamura, E. *J. Am. Chem. Soc.* **2004**, *126*, 6287−6293. (c) Nakanishi, W.; Yamanaka, M.; Nakamura, E. *J. Am. Chem. Soc.* **2005**, *127*, 1446−1453. (d) Nakamura, E.; Yamanaka, M.; Mori, S. *J. Am. Chem. Soc.* **2000**, *122*, 1826−1827. (e) Yamanaka, M.; Nakamura, E. *J. Am. Chem. Soc.* **2005**, *127*, 4697−4706. (f) Yamanaka, M.; Nakamura, E. *Organometallics* **2001**, *20*, 5675−5681.

(12) (a) Arnold, L. A.; Imbos, R.; Mandoli, A.; de Vries, A. H. M.; Naasz, R.; Feringa, B. L. *Tetrahedron* **2000**, *56*, 2865−2878. (b) Alexakis, A.; Benhaim, C.; Rosset, S.; Humam, M. *J. Am. Chem. Soc.* **2002**, *124*, 5262−5263.

agreement regarding the rate-determining step. Noyori,[13a] Kitamura,[13b] and co-workers have proposed a catalytic cycle for the Cu/sulfonamide-catalyzed 1,4-addition of diethylzinc to cyclohexenone based on kinetic data and $^{12}C/^{13}C$ isotope effect studies. Their results point toward a concerted mechanism. In another report, the CA of dialkylzincs involving copper complexes of Schiff base ligands was studied by Gennari et al.[13c] The oxidative addition of a Cu-complex to cyclohexenone was proposed as the rate-limiting step in this reaction. Alternatively, Schrader and co-workers[13d] proposed, on the basis of kinetic studies in a related copper-catalyzed CA using phosphorus ligands, a different mechanism involving a reductive elimination as the rate-limiting step.

Thus far, a detailed mechanistic study of the copper-catalyzed CA of Grignard reagents is lacking. A single, general mechanism for the catalytic CA of different organometallic reagents may not be possible due to the sensitivity of the CA reaction to almost any variation in the reaction parameters (i.e. ligand, copper source, solvent, temperature). The difficulties in mechanistic interpretations are complicated further by the absence of structural information regarding the intermediate species under catalytic conditions.[14]

The majority of the studies related to the mechanism of the copper-catalyzed 1,4-addition postulates the transmetalation between the organometallic compounds and the copper species as the first step in the catalytic cycle. However, in the enantioselective catalytic CA, transmetalated copper intermediates derived from organometallic compounds have not been characterized to date.[15] In only one case a dramatic (107 ppm) upfield shift in the ^{31}P NMR spectra of the copper complex with a chiral diphosphite ligand was reported upon addition of Et_2Zn.[16] This shift was assigned to the presence of an *Et*−Cu species.

In the present report, we explore the mechanism of the copper-catalyzed enantioselective CA of Grignard reagents, through spectroscopic, structural, and kinetic methods. On the basis of these mechanistic studies we identify catalytically active species and propose a possible catalytic cycle that is consistent with the results observed in enantioselective CA.

Results and Discussion

In our earlier communication[7c] we demonstrated that equally high enantioselectivity can be obtained by using either preformed, air-stable Cu-complexes **1a** and **2a** or the same complexes prepared in situ from the chiral diphosphine ligands (**L1** and **L2**) and CuBr·SMe_2 (Scheme 3). Furthermore, we have shown that these copper complexes could be recovered easily and reused without loss in catalytic activity.

Scheme 3. Formation of the Copper (I) Diphosphine Complexes

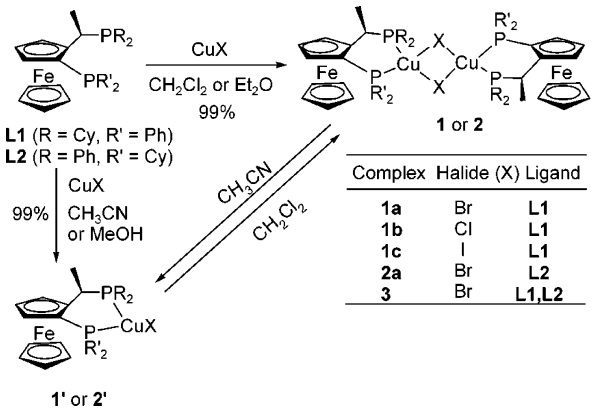

Thus, prior to discussing the species which are present during catalysis, it is pertinent to consider first the formation and properties of the copper(I) phosphine complexes employed and their dynamic behavior in solution. An interesting aspect of this class of complex is the rapid equilibration to form either a mononuclear (**1′** and **2′**) or a binuclear complex (**1** and **2**), depending on the solvent employed (Scheme 3).

Structures of the Cu−Halide complexes. The air-stable copper complexes are prepared by addition of equimolar amounts of a copper(I) salt and the chiral ligands **L1** or **L2**, respectively, in the appropriate solvent (Scheme 3). Interestingly, a solvent-dependent equilibrium between dinuclear (**1**) and a mononuclear (**1′**) species is established in solution.[7c] For example, the preparation of the bromide complex from CuBr·SMe_2 and **L1** using ethereal (Et_2O, ^{t}BuOMe) or halogenated (CH_2Cl_2, $CHCl_3$) solvents led to the dinuclear structure **1a**, as deduced by ESI-MS and IR spectroscopy.[17a] Attempts to obtain crystals suitable for X-ray analysis of **1a** from these solvents (Et_2O, ^{t}BuOMe, CH_2Cl_2), commonly used in the CA of Grignard reagents,[7a−d] were unsuccessful thus far.

In a similar manner, the dinuclear complex **2a** was prepared from CuBr·SMe_2 and **L2** in ^{t}BuOMe. Suitable crystals for X-ray analysis of this complex were obtained from an Et_2O solution. The asymmetric unit consists of one moiety of a dinuclear copper complex, which is bridged by two Br atoms resulting in a C2-symmetric unit. A molecule of the water is also present in the cell (Figure 2). The dimeric structure of **2a** in ^{t}BuOMe,

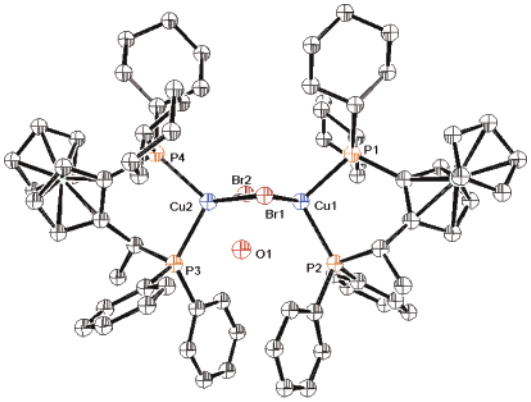

Figure 2. X-ray structure of (*S*,*R*)-**2a** (hydrogen atoms are omitted for clarity).

(13) To date only four mechanistic studies on copper-catalyzed CA of organozinc reagents have been reported: (a) Kitamura, M.; Miki, T.; Nakano, K.; Noyori, R. *Bull. Chem. Soc. Jpn.* **2000**, *73*, 999−1014. (b) Nakano, K.; Bessho, Y.; Kitamura, M. *Chem. Lett.* **2003**, *32*, 224−225. (c) Gallo, E.; Ragaini F.; Bilello, L.; Cenini, S.; Gennari, C.; Piarulli, U. *J. Organomet. Chem.* **2004**, *689*, 2169−2176. (d) Pfretzschner, T.; Kleemann, L.; Janza, B.; Harms, K.; Schrader, T. *Chem.−Eur. J.* **2004**, *10*, 6049−6057.

(14) Two structural types of organocuprates formed by the addition of Grignard reagents to a Cu(I) source, in a 1:1 ratio, have been proposed; e.g. a "RCu·MgX_2"[14a] species and an *ate* complex "R(X)CuMgX".[14b] The latter is considered more relevant and has been proposed in the related 1,4-additions of allylic copper species prepared from Grignard reagents. (a) Alexakis, A.; Commercon, A.; Coulentianos, C.; Normant, J. F. *Pure Appl. Chem.* **1983**, *55*, 1759−1766. (b) Lipshutz, B. H.; Hackmann, C. *J. Org. Chem.* **1994**, *59*, 7437−7444.

(15) Hypothetical structures of the species formed by transmetalation (with organomagnesium, organolithium, or organoaluminum compounds) of copper complexes bearing chiral ligands only have been proposed for enantioselective CA.[12] In contrast, a number of studies have been reported towards elucidation of the structures of nonchiral transmetalated copper salts (organocuprates).[8a,10,14]

(16) Yan, M.; Yang, L.; Wong, K.; Chan, A. S. C. *Chem. Commun.* **1999**, 11−12.

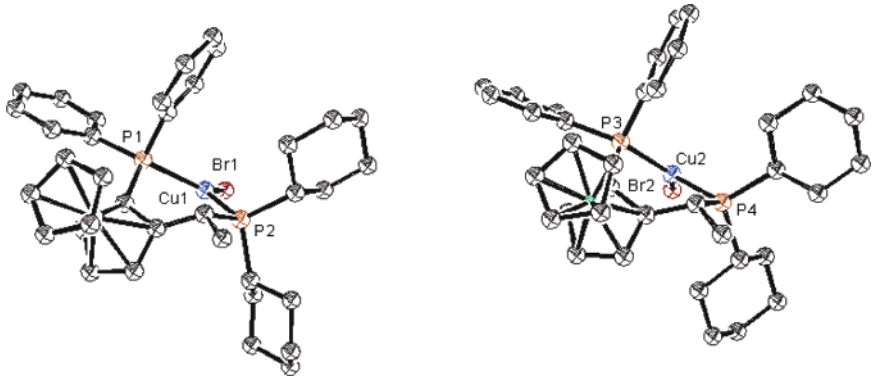

Figure 3. X-ray structure of **1a′** (hydrogen atoms are omitted for clarity).

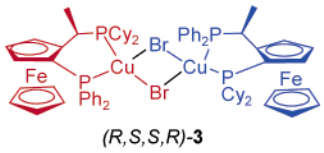

(R,S,S,R)-**3**

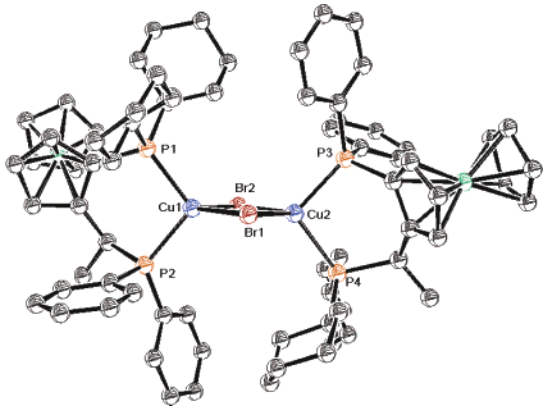

Figure 4. X-ray structure of (*R,S,S,R*)-**3** (hydrogen atoms are omitted for clarity).

CH_2Cl_2 and Et_2O solutions was also confirmed by ESI-MS.[17b] In a similar manner the preparation of copper chloride and copper iodide complexes from **L1** (Scheme 3) in halogenated solvents led to the formation of dinuclear complexes **1b** and **1c**. The dimeric structure of **1b** and **1c** in CH_2Cl_2 was confirmed by ESI-MS.

A different behavior, however, was observed when these complexes were prepared in more polar solvents, such as CH_3CN (or MeOH). Thus, the mixture of CuBr and **L1** in CH_3CN led to the formation and precipitation of the mononuclear complex **1a′**. This mononuclear Cu-complex **1a′** can be prepared by dissolving the dinuclear complex **1a** in CH_3CN also (by ESI-MS and IR).[7c] In contrast to the dinuclear complex **1a**, the mononuclear complex **1a′** is insoluble in Et_2O and ^{t}BuOMe. However, in halogenated solvents, such as CH_2Cl_2 or $CHCl_3$, **1a′** dissolves readily yielding the dinuclear complex **1a** (Scheme 3). Interestingly, both **1a′** and **1a** in CD_3CN and CD_2Cl_2, respectively, showed nearly identical ^{1}H and ^{31}P NMR spectra, thus, precluding the use of NMR spectroscopy to distinguish mono- or dinuclear structures. Further evidence of the monomeric structure of **1a′** was obtained by X-ray diffraction of crystals obtained by slow evaporation of a CH_3CN solution.

The crystal structure shows a trigonal planar mononuclear Cu-complex **1a′** (Figure 3). No solvent molecules are coordinated to the copper center. The asymmetric unit consists of two molecules of the monomeric complex **1a′**. The difference between the two molecules in the unit cell is due to a conformational change in the dicyclohexyl moieties. In the crystal structure copper exhibits distorted trigonal coordination geometry with the copper ion bound to two phosphorus and one bromide atoms. The metal forms a six-member chelate ring with the ligand, in a boatlike conformation.

The propensity of the Cu complexes of **L1** and **L2** to form dinuclear structures in solvents used in the CA reaction (Et_2O, CH_2Cl_2, ^{t}BuOMe) is demonstrated also by the formation of the stable heterocomplex **3** (Figure 4).

Complex **3** was prepared by mixing, (*R,S*)-**L1**, (*S,R*)-**L2**, and CuBr·SMe_2 in ratio 1:1:2 in CH_2Cl_2. Complete formation of the heterocomplex **3** was monitored by TLC.[17c] The dinuclear structure of heterocomplex **3** was confirmed by X-ray analysis (Figure 4). The asymmetric unit consists of one molecule of dinuclear Cu-complex **3** and two highly disordered hexane solvent molecules.

In conclusion, in solution the copper complexes exhibit a mononuclear structure in CH_3CN and MeOH, while in ethereal and halogenated solvents the dinuclear structure is dominant. Importantly, the mononuclear complex is insoluble in ethereal solvents and dissolves in the halogenated solvent due to its rapid conversion to the dinuclear form.

Redox Properties of Cu−Halide Complexes. It is apparent from our earlier reports[7a−c] that there is a considerable sensitivity of the outcome of the copper(I)-catalyzed, enantioselective CA of Grignard reagents to the nature of the ligand and substrate class employed. This sensitivity is expected to arise from both steric and electronic differences between the various Cu(I) diphosphine complexes. Electrochemistry represents a powerful tool in probing the electronic properties of redox active systems, and in the present study, it enables a direct measurement of the

(17) (a) For full spectroscopic details, see ref 7c. (b) See Supporting Information. (c) The R_f value for the heterocomplex **3** is different from the R_f value of the dinuclear complexes **1a** and **2a**.

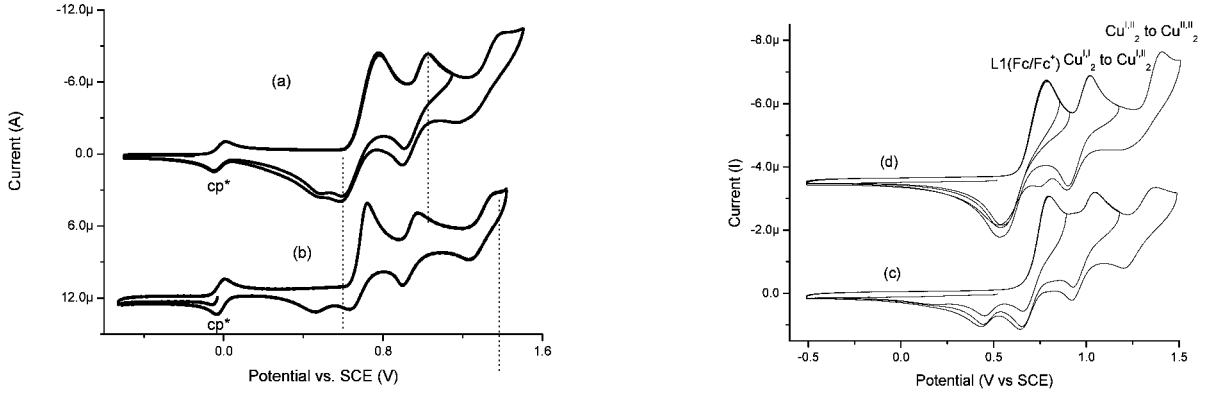

Figure 5. (Left) Oxidative electrochemistry of (a) **1a** and (b) **2a** in CH_2Cl_2 (0.1 M $TBAPF_6$) at −78 °C, scan rate = 25 mV s^{-1}. (Right) Oxidative electrochemistry of (c) **1b** (Cl^-), (d) **1c** (I^-) in CH_2Cl_2 (0.1 M $TBAPF_6$) at −78 °C, scan rate = 50 mV s^{-1}.

different electronic properties of the copper(I) complexes (**1**, **2**) and, in particular, the effect of ligand and halide variation.

The electrochemical properties of the copper(I) complexes of the ligands **L1** and **L2** both prepared in situ and as preformed complexes were investigated (Figures 5, 6).[18a] At room temperature, in MeCN or CH_2Cl_2 (0.1 M $TBAPF_6$) all complexes exhibit a single reversible oxidation at ∼0.65 V (vs SCE) assigned to the ferrocene component of the ligand and additional ill-defined redox chemistry at more anodic potentials assigned to irreversible Cu(II)/Cu(I) redox processes.

Importantly, for the free ligands, **L1** and **L2**, an irreversible oxidative process is observed prior to the ferrocene oxidation allowing for facile detection of free ligand in solution. This process is assigned to oxidation of the phosphine moieties of the ligands. At lower temperature (−78 °C), the redox process of the free ligand shows some reversibility indicating that the irreversible oxidation is due to an EC mechanism (i.e. the electrochemical oxidation is followed by a chemical reaction).[18b,c] The absence of this process in the voltammetry of the copper complexes formed both in situ and ex situ confirms that copper(I) coordinates to the ligands in a 1:1 ratio and that the formation constant is very high.

In contrast to ambient conditions, at lower temperatures (e.g., −20 to −80 °C) a considerable improvement in the reversibility of the Cu(II)/Cu(I) redox processes of the complexes is observed (Figure 5). For both **1a** and **2a** electrochemically reversible processes are observed at ∼0.70 [2 e^-], 0.95 [1 e^-], and 1.30 [1 e^-] V (vs SCE). The bielectronic nature of the first redox process is assigned on the basis of both the intensity of the anodic wave relative to the two subsequent anodic waves and on the presence of two return waves of equal intensity. The presence of two one-electron Cu(II)/Cu(I) redox processes supports the assignment of the solution structure in CH_2Cl_2 as being a dinuclear halide-bridged complex (Figure 5, left: a, b).

For both **1a** and **2a** the first oxidation wave corresponds to single-electron oxidations of each of the ferrocene units of the binuclear complex (Figure 5, left). That at least one of the oxidations is electrochemically reversible is clear from the separation ($E_{p,a} - E_{p,c}$), which is close to the 59 mV associated with ideal Nernstian behavior. As the temperature is increased, the two return waves become a single reversible redox wave (vide supra).

Surprisingly, the chloro, bromo, and iodo **(1a−c)** complexes give almost identical electrochemistry with the exception of the ferrocenium reduction, in which a decrease in the separation of the first and second reductive processes (at ∼0.5 V) is observed on going from chloro to bromo to iodo (Figure 5, respectively c, a, d).

For the halide-free complex **4** prepared in situ from [Cu(I)-$(CH_3CN)_4$]PF_6 and **L2** (1:1), no evidence of free ligand or oxidative instability was observed at −70 °C in CH_2Cl_2. In contrast to the halide-based complexes two electrochemically reversible 1 e^- processes are observed (Figure 6).[18d] The first oxidation (assigned to the ferrocene redox couple of the coordinated ligand) is similar to that observed for the halide complexes; however, only a single reductive ferrocenium/ferrocene wave is observed. The Cu(II)/Cu(I) redox process is considerably more anodic than that observed for both of the copper-based oxidation steps in the halide complexes. This is as expected, considering the weaker donor strength of MeCN in comparison to that of Cl^- and Br^-. Addition of 1 equiv of TBABr to the CH_2Cl_2 solution resulted in a dramatic change to the cyclic voltammetry with the appearance of new redox waves at positions identical to that observed for **2a** and a reduction in the reversibility of the ferrocene redox process with a second ferrocenium reduction wave being observed (Figure 6). This confirms that the binuclear halide-bridged complex is the thermodynamically most favored complex in halogenated solvents.

Although overall similar electrochemical behavior is observed for all complexes, the potentials of the two Cu(II)/Cu(I) redox processes and the separation of the first and second ferrocenium reductions is dependent on the ligand involved. This demonstrates clearly that, although all of the complexes examined are, essentially, structurally similar, the electron density on the copper(I) centers is distinctly different in each case.

The identification of significant differences in the redox properties of the copper(I) centers with ligand variation suggests that electronic factors may play an important role in determining the specificity of the ligands to particular substrate classes. For example, in comparison to **1a**, complex **2a** was found to be more selective toward nonactivated substrates.[7c] From electrochemistry, it is apparent that **2a** is easier to oxidize and hence

(18) (a) For the electrochemistry measurements of the copper complexes and free ligands performed at room temperature, see Supporting Information. (b) Ong, J. H. L.; Nataro, C.; Golen, J. A.; Rheingold, A. L. *Organometallics* **2003**, *22*, 5027−5032. (c) Pinto, P.; Calhorda, M. J.; Felix, V.; Aviles, T.; Drew, M. G. B. *Monatsh. Chem.* **2000**, *131*, 1253−1265. (d) The halide-free copper complex **4**, prepared from equimolar amounts of **L1** and $[Cu(CH_3CN)_4]PF_6$, provides similar catalytic activity for the enantioselective conjugate addition of Grignard reagents to enoates. Complex **4** was prepared only in situ due to instability in solid state.

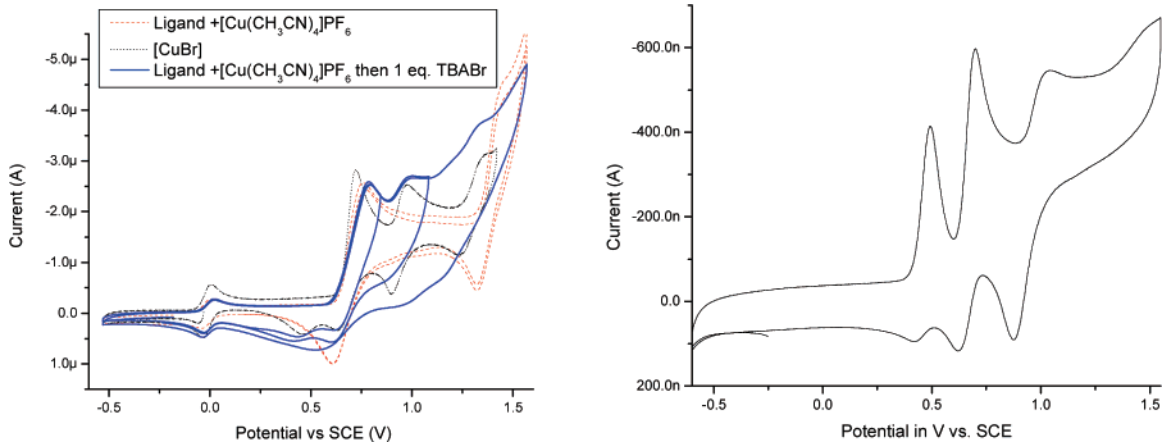

Figure 6. Oxidative electrochemistry (at −78 °C) of (left) **L2**/[Cu(I)$(CH_3CN)_4$]PF_6 (1:1, red) in CH_2Cl_2 (0.1 M $TBAPF_6$), in the presence of 1 equiv of TBABr (blue) and the oxidative electrochemistry of **2a** (black) at −78 °C, scan rate = 25 mV s^{-1}; and of (right) **L2** in CH_2Cl_2 (0.1 M $TBAPF_6$). Scan rate = 25 mV s^{-1}

Scheme 4. CA of MeMgBr to Octenone **5**[a]

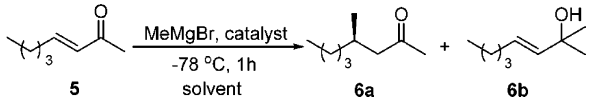

5 **6a** **6b**

[a] Reagents and conditions: (1) uncatalyzed reaction MeMgBr (1.5 equiv). (2) Racemic series: CuBr·SMe_2 (5 mol %); MeMgBr (1.5 equiv). (3) Enantioselective series: **1a**−**c** (5 mol %); MeMgBr (1.1 equiv).

Table 1. CA of MeMgBr to Octenone **5**

entry	[Cu] [5 mol %]	solvent	conv. [%][a]	**6a**:**6b**[a]
1[b]	–	Et_2O	52	1:99
2[b]	–	CH_2Cl_2	55	1:99
3[c]	CuBr·SMe_2	Et_2O	88	55:45
4[c]	CuBr·SMe_2	CH_2Cl_2	85	42:58

[a] Conversion and regioselectivity were determined by GC. [b] Conditions (1), Scheme 4, reaction time 1 h, **5** (0.35 M). [c] Conditions (2), Scheme 4, reaction time 1 h, **5** (0.35 M).

is more electron rich than **1a**. Hence, the difference in reactivity may be related to the energy match of substrate and catalyst. However, further investigation over a broader range of catalysts is necessary to determine if a correlation between measured redox potentials and substrate specificity is justifiable. Nevertheless, the present results indicate that such a correlation is plausible.

The Influence of the Solvent and Halide on the Enantioselective CA Reaction. Having established the structures and basic redox properties of the initial copper complexes, a more detailed examination of the various reaction parameters was performed. Previously, we have demonstrated the importance of carrying out the reaction at low temperature to achieve good levels of regio- and enantioselectivity;[7b−d] hence, in the present study reactions were carried out at −78 °C.

As a model system for the present study we choose the CA of MeMgBr to octenone **5** under three different sets of conditions (Scheme 4): (1) in the absence of catalyst, (2) using 5 mol % of CuBr·SMe_2 (racemic series), (3) in the presence of 5 mol % of chiral complexes **1a**−**c** (enantioselective series). MeMgBr was employed as the Grignard reagent in this reaction to take advantage of its relatively low reactivity. The decreased reactivity of MeMgBr compared to those of its homologues is attributed to the significantly higher strength of the C−Mg bond (MeMgBr > 250 kcal/mol > EtMgBr ≥ PrMgBr ≥ BuMgBr > 200 kcal/mol > ^{t}BuMgBr).[19] Initially, we determined the conversion and regioselectivity of the CA of the MeMgBr to **5** in the absence of catalyst, and catalyzed by CuBr·SMe_2 (in CH_2Cl_2 and Et_2O) (Scheme 4, Table 1).

Table 2. Enantioselective CA of MeMgBr to **5** Catalyzed by 5 mol % Copper Bromide Complex **1a**[a]

entry	solvent	conv. [%][b]	**6a**:**6b**[b]	ee[%][c]
1	CH_2Cl_2	88	86:14	92
2	toluene	89	88:12	91
3	^{t}BuOMe	90	97:3	96
4	Et_2O	87	83:17	87
5	THF	67	2:98	2
6[d]	CH_2Cl_2	35	75:25	80
7[e]	CH_2Cl_2	25	42:58	75

[a] Reaction conditions: reaction time 1 h, **5** 0.35 M, MeMgBr 1.5 equiv, −78 °C. [b] Conversion and regioselectivity determined by GC. [c] Determined by GC (chiral dex-CB column). [d] Dioxane (1 equiv) was added to the mixture of catalyst and MeMgBr in CH_2Cl_2 prior to addition of **5**. [e] Me_2Mg (1.5 equiv) was used instead of MeMgBr for this reaction.

As expected, the addition of MeMgBr to enone **5** at −78 °C in Et_2O led to the 1,2-addition product **6b** as the major compound with 52% conversion in 1 h (Table 1, entry 1). Similar results were obtained in CH_2Cl_2 (entry 2). Employing a catalytic amount of CuBr·SMe_2 under the same conditions provided higher conversion and afforded the 1,4-addition product **6a** with modest regioselectivity (entries 3, 4).

Enantioselective Series: Solvent Dependence. Table 2 summarizes the results obtained in the CA of MeMgBr to **5** catalyzed by chiral copper catalyst **1a** and the solvent dependence observed. The reaction proved to be remarkably tolerant to a range of solvents (Table 2, entries 1−3). For instance, in CH_2Cl_2 and toluene **6a** was obtained in excellent yield and with high regio- and enantioselectivity (entries 1, 2).

In ethereal solvents high regio- and enantioselectivity was observed also, albeit with higher selectivity in ^{t}BuOMe than in Et_2O (entries 3, 4). Interestingly, employing THF as a solvent resulted in a significant decrease in the rate of the reaction and a near complete loss of regio- and enantioselectivity (2% ee), (entry 5).

We reasoned that the Schlenk equilibrium[20] could be the most important factor in determining the solvent dependence in the

(19) Silverman, G. S., Rakita, P. E., Eds. *Handbook of Grignard Reagents*; Marcel Decker Inc.: New York, 1996.
(20) Schlenk, W.; Schlenk, Jr. *Ber. Dt. Chem. Ges.* **1929**, *62B*, 920−924.

Table 3. CA of MeMgX to **5** Catalyzed by 5 mol % Copper Complex **1** in CH_2Cl_2[a]

entry	CuX	1	MeMgX	conv. [%][b]	**6a:6b**[b]	ee [%][c]
1	CuBr	**1a**	MeMgBr	88	86:14	92
2	CuCl	**1b**	MeMgBr	95	85:15	94
3	CuI	**1c**	MeMgBr	85	85:15	90
4	CuBr	**1a**	MeMgCl	88	82:18	91
5	CuCl	**1b**	MeMgCl	99	50:50	72
6	CuBr	**1a**	MeMgI	94	77:23	30
7	CuI	**1c**	MeMgI	95	71:29	36

[a] Reaction conditions: reaction time 1 h, **5** (0.35 M), MeMgBr 1.5 equiv, −78 °C. [b] Conversion and regioselectivity determined by GC. [c] Determined by GC (chiral dex-CB column).

CA of MeMgBr. Benn and co-workers[21a] demonstrated that the Schlenk equilibrium between EtMgBr and Et_2Mg in Et_2O favored the solvent-coordinated monoalkylmagnesium species $EtMgBr{\cdot}OEt_2$. By contrast, in THF, R_2Mg and $MgBr_2$ are the dominant species present in solution.[21b] Furthermore, it is known that the Schlenk equilibrium can be driven, partially, toward the formation of R_2Mg in any solvent by the addition of dioxane to a solution of the Grignard reagent.[22]

Two different experiments were performed to establish whether the involvement of the Me_2Mg species in THF could be responsible for the decrease in the rate and enantioselectivity of the reaction. (1) Addition of 1 equiv of dioxane to a mixture of **1a** and MeMgBr in CH_2Cl_2 prior to addition of substrate **5** had a dramatic, negative, effect on the reaction, providing product **6a** with low conversion and with a significant decrease in enantioselectivity (entry 6).[23a] (2) The involvement of the Schlenk equilibrium in THF was supported further by the direct use of Me_2Mg instead of MeMgBr. The CA of Me_2Mg to **5** in CH_2Cl_2, led to the product with low conversion and modest enantioselectivity (entry 7), similar to that observed in the presence of dioxane.[23b]

Halide Dependence. The CA to **5** employing different combinations of CuX and MeMgX was examined to explore the effect of halide on the outcome of the reaction (Table 3).[24a] It is apparent that the CA reaction is dependent both on the nature of the halide present in the Grignard reagent and in the Cu(I) salt (Table 3). The presence of bromide, either in the Grignard reagent or in the copper salt, is essential to achieve full conversion and high regio- and enantioselectivity. For instance, the combination of MeMgBr with the copper chloride complex **1b** or the copper iodide complex **1c** provided product **6a** with high regio- and enantioselectivity in both cases, comparable with results using CuBr (entries 1−3). In a similar manner the CA of MeMgCl to **5** catalyzed by **1a** proceeds with high regio- and enantioselectivity (entry 4).

However, the use of MeMgCl together with CuCl resulted in a significant decrease in the enantioselectivity from 92% to 72% ee. In addition, the regioselectivity decreased (entry 5). Furthermore, when MeMgI was used in combination either with **1a** or **1c**, low enantioselectivity, accompanied with a noticeable decrease in the regioselectivity was observed (entries 6, 7).[24b]

^{1}H NMR and ^{31}P NMR Spectroscopy. From ESI-MS, IR spectroscopy, X-ray crystallography, and electrochemistry studies, the copper complexes **1a** and **2a** exist as bromide-bridged dinuclear complexes in the solvents used in the CA reaction (CH_2Cl_2, Et_2O, ^{t}BuOMe). However, the copper−halide complexes studied in this asymmetric CA are precursors to the catalytically active species generated upon addition of the Grignard reagents. By analogy with the formation of an organocuprate via transmetalation of an organometallic reagent with a copper source, it is proposed that a similar process occurs upon addition of Grignard reagents to the Cu−halide complexes.[14] To detect and characterize the reaction intermediates in the present system, a detailed NMR spectroscopic study was performed.

First, complexes **1a**−**c** were investigated in solution prior to addition of both the Gringard reagent and the enone. The ^{1}H NMR and ^{31}P NMR spectra of complex **1a** in CD_2Cl_2 are presented in Figure 7a. ^{31}P NMR shows two doublets with a J_{P-P} = 186 Hz corresponding to the dicyclohexyl (8.21 ppm) and diphenylphosphine (−24.06 ppm) groups.[25] Variable-temperature ^{1}H NMR spectroscopy showed a slight variation in the chemical shifts of the aromatic protons. Particularly, the absorption at 7.0 ppm corresponding to two ortho protons of the phenyl group, observed at low temperature (below −30 °C) was shifted downfield at RT and overlapped with the signal at 7.2 ppm. ^{31}P NMR did not reveal significant temperature-dependent changes in the chemical shifts of **1a**.

To determine the structure of the species formed during the reaction, complex **1a** and an excess (1.5−10.0 equiv) of MeMgBr were mixed in CD_2Cl_2 at −78 °C, and the resulting mixture was studied by NMR spectroscopy at −60 °C. ^{31}P NMR spectroscopy showed upfield shifts of both phosphorus resonances (Figure 7b). In the ^{31}P NMR two doublets corresponding to dicyclohexyl (6.41 ppm) and diphenylphosphine (−27.13 ppm) moieties were shifted by 1.8 ppm and 3.1 ppm, respectively, relative to those of the initial complex **1a**, indicating the formation of a new species, **A**.[26] These chemical shifts can be compared with the large ^{31}P NMR upfield shift, assigned by Chan and co-workers to a $(L)_nCuEt$ species, generated from Et_2Zn, $Cu(OTf)_2$, and a phosphine ligand.[16]

In the present study, the value of the P−P coupling constant changed from J_{p-p} = 186 Hz in the initial complex **1a** to J_{p-p} = 143 Hz. Formation of **A** was confirmed by ^{1}H NMR spectroscopy also (Figure 7b). A new sharp singlet was observed at −0.3 ppm, which is attributed tentatively to a Cu*Me* species.[27]

(21) (a) Benn, R.; Lehmkuhl, H.; Mehler K.; Rufińska, A. *Angew. Chem., Int. Ed. Engl.* **1984**, *23*, 534−535. (b) Smith, M. B.; Becker, W. E. *Tetrahedron* **1966**, *22*, 3027−3036.

(22) Dioxane is a common reagent for synthesis of R_2Mg from RMgX due to irreversible coordination with MgX_2. For the synthesis of R_2Mg, see: (a) Tadeusz, F.; Molinski, T. F.; Ireland, C. M. *J. Org. Chem.* **1989**, *54*, 4256−4259. (b) von dem Bussche-Hünnefeld, J. L.; Seebach, D. *Tetrahedron* **1992**, *48*, 5719−5730.

(23) (a) Significant precipitation, observed after addition of dioxane to the mixture of catalyst with Grignard reagent, was attributed to a complex of dioxane with $MgBr_2$. (b) Solvent- and halide-dependent experiments were performed on the CA of EtMgX to methyl crotonate also. For the results, see Supporting Information.

(24) (a) Similar results were obtained employing both preformed and prepared in situ copper complexes. (b) Explanation for the results obtained with MeMgI arose from the NMR studies, vide infra.

(25) The saturation ^{31}P NMR experiments and phase-sensitive phosphor−phosphor COSY spectrum (for the spectrum see Supporting Information) showed no passive coupling to the copper, indicating only phosphorus−phosphorus coupling. Attempts to observe ^{63}Cu NMR spectra were unsuccessful possibly due to fast quadrupolar relaxation and broken symmetry (see refs 29 a and c).

(26) (a) Employing 1 equiv of MeMgBr did not provide complete formation of the new species **A**. (b) When the CA to octenone **5** was performed in Et_2O, a significant amount of a precipitate was observed after the addition of MeMgBr to **1a**, and prior to the addition of the enone. This suggests that the newly formed species is not soluble in Et_2O. (c) Attempts to crystallize species **A** were unsuccessful.

(27) Besides the signal attributed to the CuMe group, another singlet at δ 1.64 ppm was detected and assigned to the excess of MeMgBr used in these experiments. For a full range of the NMR spectra, see Supporting Information.

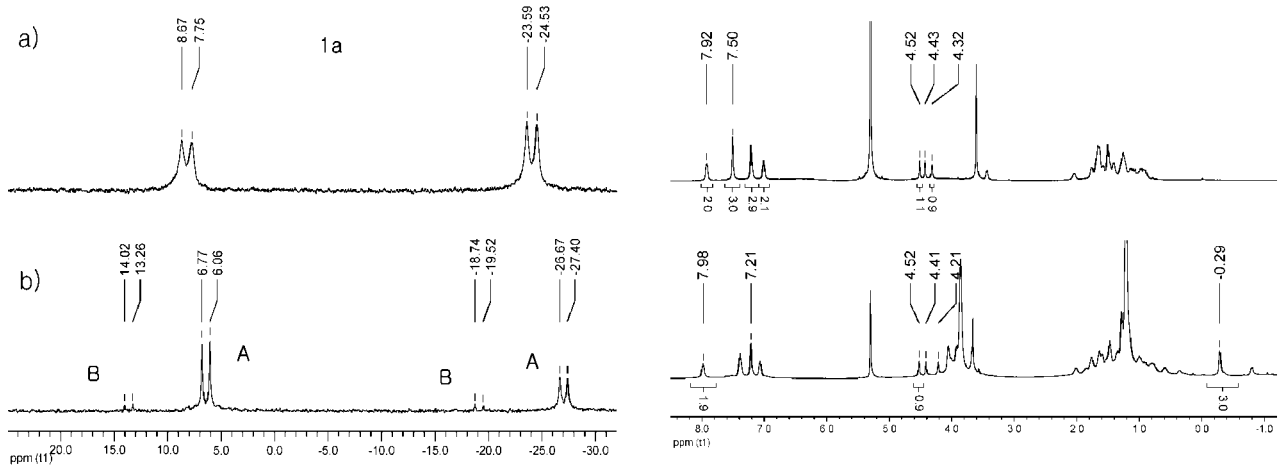

Figure 7. ^{31}P NMR (left) and ^{1}H NMR (right) spectra in CD_2Cl_2 at −60 °C: (a) complex **1a**, (b) complex **1a** with 3 equiv of MeMgBr.

Chart 1. Structures Proposed for the Alkyl Copper(I) Complexes

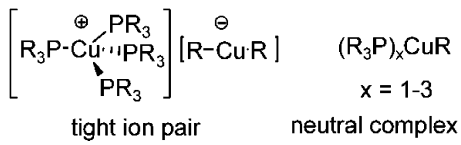

The integration indicates that only 1 methyl group is bound to the copper, even in the presence of up to 10 equiv of MeMgBr. The observed Cu*Me* shift may be compared with the ^{1}H NMR absorptions of related achiral alkylcopper species "$(PR_3)_x$CuMe" for which chemical shifts of +0.3 to −1.0 ppm were reported previously.[28]

The dynamic equilibrium of the newly formed species **A** was studied by variable-temperature ^{31}P NMR spectroscopy. No changes in the spectra were observed over the temperature range −30 to −78 °C. Moreover, species **A** proved to be stable in solution at these temperatures under an inert atmosphere for several days. However, increasing the temperature to 23 °C resulted in decomposition of **A**, with concomitant formation of a black precipitate due to release of metallic copper. Despite this instability in CD_2Cl_2 at RT, species **A** proved to be more stable in Et_2O, and no decomposition was detected over 30 min at room temperature.[26b,c]

As can be seen in Figure 7, the formation of species **A** in CD_2Cl_2 was accompanied by the appearance of traces of two new doublets (species **B**) in the ^{31}P NMR spectrum at 13.6 and −19.1 ppm (vide infra). The importance of this species in the CA reaction will be discussed below.

On the basis of literature precedents, several structures can be proposed for species **A**. Thus, alkyl copper(I) complexes of achiral phosphine ligands with the general structures presented in Chart 1 were proposed previously on the basis of spectroscopic data and X-ray structure analysis.[28a−c,29]

The general procedure applied for the synthesis of the complexes presented in Chart 1 differs from the one used in the present study by the order of addition and reacting components. The experimental procedures reported previously were based on the direct reaction of organometallic compounds (Me_2AlOEt, MeLi, Me_2Mg) with Cu(II) salts and phosphine ligands,[28,29] whereas in our case the synthesis of the alkyl copper complexes is carried out by the addition of organometallic reagents to the preformed copper(I) bromide complexes of diphosphine ligands (**L1**, **L2**) (vide supra).

To establish whether the species observed in our system are analogous to the complexes shown in Chart 1, the preparation of species **A** directly from the free ligand **L1**, a copper(II) salt and the Grignard reagent was attempted following literature procedures.[28,29] Unfortunately, clear results from these experiments were not obtained due to the appearance of a number of new signals indicating formation of several complexes, whereas no trace of species **A** was observed.

Alternatively, we wondered whether the species **A** might be generated by using MeLi instead of MeMgBr. Interestingly, the addition of 1.0−2.0 equiv of MeLi to **1a,** at −78 °C in CD_2Cl_2, led to the formation of a single, new copper species **C** (Figure 8b).

Two doublets in the ^{31}P NMR spectrum appeared at 11.61 ppm and −25.44 ppm (J_{p-p} = 163 Hz) with concomitant disappearance of the characteristic signals of **1a**.[30a] The ^{1}H NMR absorption of Cu*Me* appeared at −0.77 ppm, which was shifted upfield by 0.49 ppm with respect to **A**. Interestingly, addition of more than 2 equiv of MeLi to **1a** led to the formation of **C**, with simultaneous decomplexation of the ligand **L1** (−28.5 ppm in the ^{31}P NMR spectrum, Figure 8b) and formation of $LiCuMe_2$ (detected in the ^{1}H NMR spectrum, −1.17 ppm).[30b]

The roles of Mg^{2+} and Li^{+} ions in the structures of **A** and **C**, respectively, were investigated by addition of selective additives to remove those ions from the coordination sphere of the copper atom. Addition of 1.5 equiv of 12-crown-4 to a solution of **C** (formed by addition of 1.5 equiv MeLi at −78 °C in CH_2Cl_2)

(28) (a) Dempsey, D. F.; Girolami, G. S. *Organometallics* **1988**, *7*, 1208−1213. (b) House, H. O.; Fischer, W. F. *J. Org. Chem.* **1968**, *33*, 949−956. (c) Miyashita, A.; Yamamoto, A. *Bull. Chem. Soc. Jpn.* **1977**, *50*, 1102−1108. (d) Ikariya, T.; Yamamoto, A. *J. Organomet. Chem.* **1975**, *72*, 145−151. (e) Pasynkiewicz, S.; Poplawska, J.; *J. Organomet. Chem.* **1985**, *282*, 427−434. (f) Pasynkiewicz, S.; Pikul, S.; Poplawska, J. *J. Organomet. Chem.* **1986**, *293*, 125−130.

(29) (a) Gambarotta, S.; Strologo, S.; Floriani, A.; Chiesi-Villa, A.; Guastini, C. *Organometallics* **1984**, *3*, 1444−1445. (b) Coan, S. P.; Folting, K.; Huffman, J. C.; Caulton, K. G. *Organometallics* **1989**, *8*, 2724−2728. (c) Schaper, F.; Foley, S. R.; Jordan, R. F. *J. Am. Chem. Soc.* **2004**, *126*, 2114−2124. (d) Mankad, N. P.; Gray, T. G.; Laitar, D. S.; Sadigi, J. P. *Organometallics* **2004**, *23*, 1191−1193.

(30) (a) The observed value of the J_{p-p} coupling constant was 20 Hz lower compared to the J_{p-p} obtained for the species **A** (J_{p-p} = 143 Hz). (b) The assignment was made by the correlation of observed chemical shift and the chemical shift reported for $LiCuMe_2$ in the literature (δ = −1.0 to δ −1.4). See: (a) Lipshutz, B. H.; Kozlowski, J. A.; Breneman, C. M. *J. Am. Chem. Soc.* **1985**, *107*, 3197−3204. (b) House, H. O.; Respass, W. L.; Whitesides, G. M. *J. Org. Chem.* **1966**, *31*, 3128−3141.

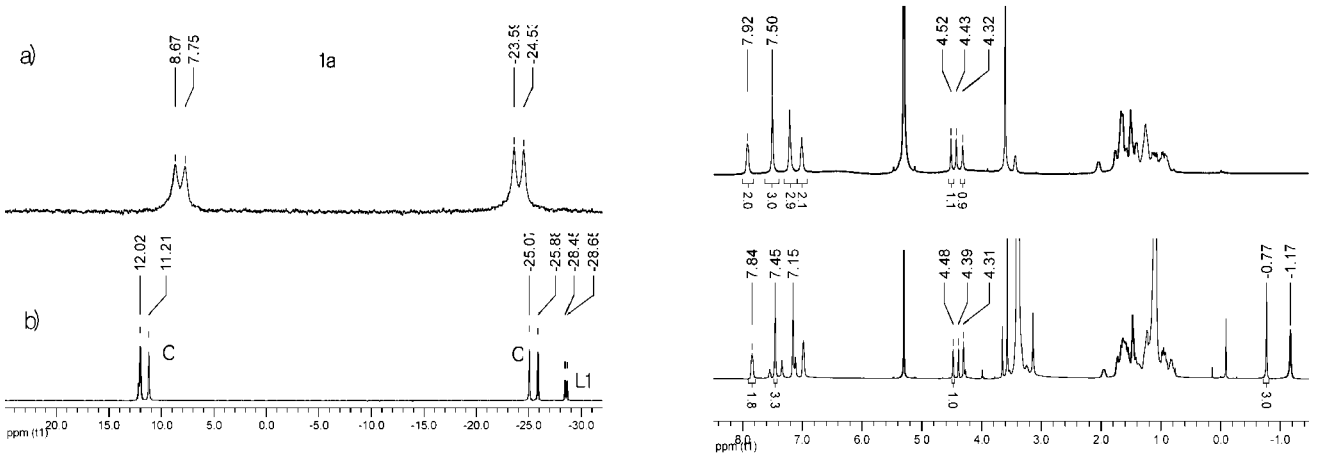

Figure 8. ^{31}P NMR (left) and ^{1}H NMR (right) spectra in CD_2Cl_2 at −60 °C: (a) complex **1a**, (b) complex **1a** with 3 equiv of MeLi (signal at δ −28.5 ppm in the ^{31}P spectrum corresponds to the free ligand **L1** usually formed when more than 2 equiv of MeLi are used).

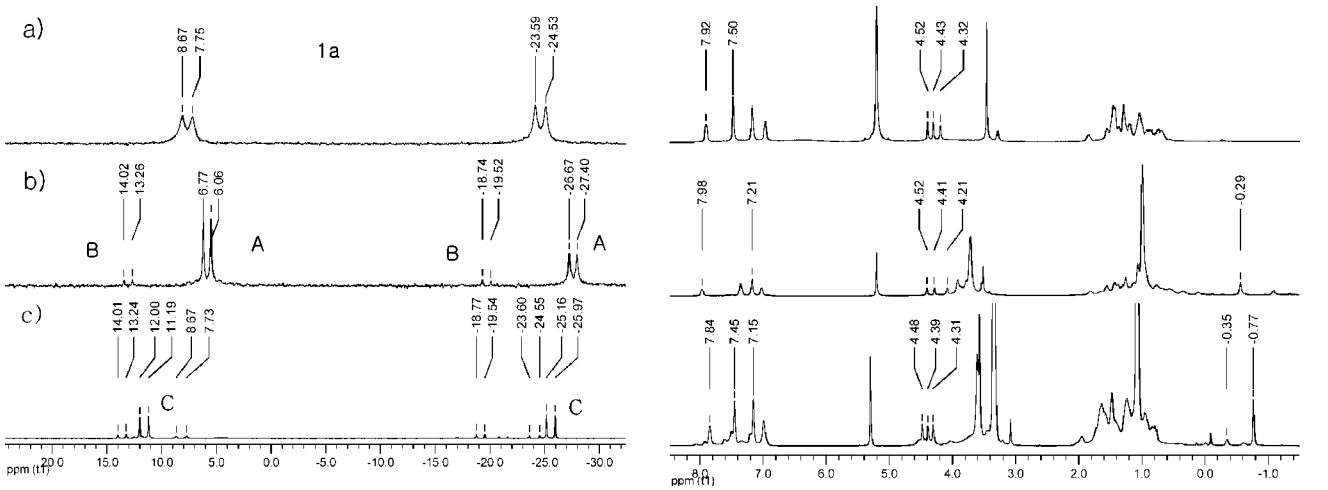

Figure 9. ^{31}P NMR (left) and ^{1}H NMR (right) spectra in CD_2Cl_2 at −60 °C: (a) complex **1a**; **(**b) complex **1a** with 3 equiv of MeMgBr; (c) complex **1a** with 3 equiv of MeMgBr followed by addition of 3 equiv of dioxane.

resulted in the formation of a precipitate; however, the ^{31}P NMR spectrum of species **C** was unaffected. This suggests that Li^+ is not involved in the structure of species **C**, i.e. Li^+ is not present within the first coordination sphere of complex **C**.

On the other hand, dioxane could be employed to drive the formation of R_2Mg from RMgX (vide supra) since it coordinates strongly to $MgBr_2$ and results in precipitation of the dioxane complex from the reaction mixture.[22] If $MgBr_2$ is part of the complex **A**, then addition of dioxane will, necessarily, have an influence on its structure.

Addition of 3 equiv of dioxane at −78 °C to a CD_2Cl_2 solution of **A** (formed by addition of 3 equiv of MeMgBr) resulted in the immediate conversion of species **A** to species **C** (Figure 9b, c), with concomitant formation of a precipitate. Importantly, it was found that the addition of Me_2Mg, instead of MeMgBr or MeLi to complex **1a** afforded **C** as the major species also.[17b]

Thus, these experimental results demonstrate clearly that $MgBr_2$ is an intimate component of the transmetalated species **A**. On the basis of these experiments, two different structures **I** or **II** (Scheme 5a) can be proposed for the species **A**, formed after addition of MeMgBr to **1**. However, the 1:1 ratio of Cu/Me revealed by ^{1}H NMR allows us to exclude **II** and to postulate **I** as the most appropriate structure for species **A**.[31]

Scheme 5. Possible Structures for the Species **A** and **C** Formed by Transmetalation of **1a** with MeMgBr and MeLi, Respectively

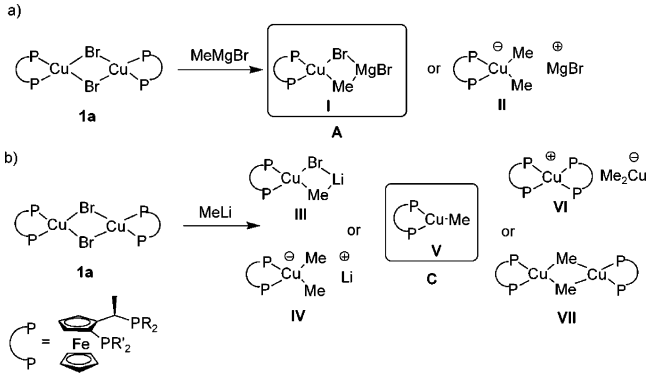

With respect to species **C**, formed upon addition of MeLi (as well as after addition of Me_2Mg) to **1a**, complexes **III** or **IV** (Scheme 5b) can be excluded due to the experimentally observed conversion of **A** to **C** upon addition of dioxane. This is supported further by the absence of an effect of 12-crown-4 ether on **C** formed after addition of MeLi, as well as by the

(31) Hence, the complex **1a** was prepared from CuBr and ligand **L1** in 1:1 ratio; consequently 1:1 ratio of *Me* to **L1**, observed in ^{1}H NMR after adding of MeMgBr, indicates that only one *Me* group is coordinated to the copper atom.

Scheme 6. Stoichiometric Addition of Octenone **5** to the Species **A** and **C**

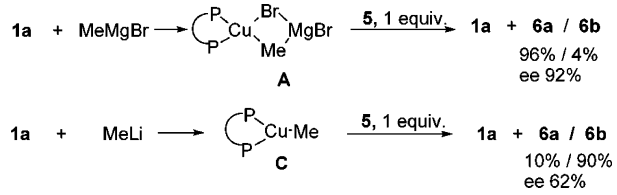

generation of **C** by addition of Me_2Mg to **1a**. One of the structures **V**−**VII**, could also be a priori attributed to **C**. Type **V** structures for alkylcopper phosphine complexes have been proposed by several groups.[28,29] On the basis of X-ray structures Girolami et al. suggested that alkylcopper complexes can adopt structure **VI**, depending on the bulkiness of phosphine ligands and alkyl group and, more significantly, the nature of the solvent (vide infra).[28a]

Nevertheless in the present case we can exclude complex **VI** as a possible structure for species **C**, as it would result in a more complicated ^{31}P NMR spectrum than those which are obtained experimentally for **C**. There are no literature precedents for the viability of the complexes of structure **VII** where alkyl groups bridge two copper centers.[32] On the basis of the data analysis given above we propose structure **I** for species **A** and structure **V** for species **C**.

To establish the relevance of species **A** and **C** in the catalytic CA we performed stoichiometric additions of octenone **5** to their solutions at −78 °C, and the changes in the resulting mixtures were followed by ^{1}H and ^{31}P NMR spectroscopy (Scheme 6).

Addition of an equimolar amount of **5** to either species **A** or **C** led to instantaneous and quantitative formation of the initial complex **1a** with concomitant formation of the addition products **6**. Addition of 1 equiv of **5** to **A** provided the 1,4-adduct **6a** with regioselectivity of 96% and 92% ee.

These values are in agreement with those obtained for the CA of MeMgBr to **5**, catalyzed by **1a** (Table 2, entry 1). In contrast, the addition of 1 equiv of **5** to **C** (obtained from MeLi) led to the 1,4-adduct **6a** with regioselectivity of 10% and enantioselectivity of 62%. Considering that species **C** can be formed by either addition of Me_2Mg to **1a** or of dioxane to **A**, the data correlates well with the low conversion and enantioselectivity obtained in the catalytic reactions performed with Me_2Mg (Table 2, entry 7) and with MeMgBr and dioxane as an additive (Table 2, entry 6). Thus, we can postulate that the generation of species **A**, rather than **C**, is essential to obtain high levels of regio- and enantioselectivity in the catalytic CA of Grignard reagents to unsaturated carbonyl compounds.

As shown in Table 2, the nature of the solvent has a significant influence on the selectivity of the reaction. Similarly, it can be expected that the nature of the solvent could lead to a preference for the formation of **A** or **C**. The influence of several solvents on the distribution of the copper species was studied by ^{31}P NMR spectroscopy (Figure 10a, b).[33]

In Et_2O and CH_2Cl_2 the Cu-complex **A** is the major component obtained after addition of MeMgBr to **1a** (vide

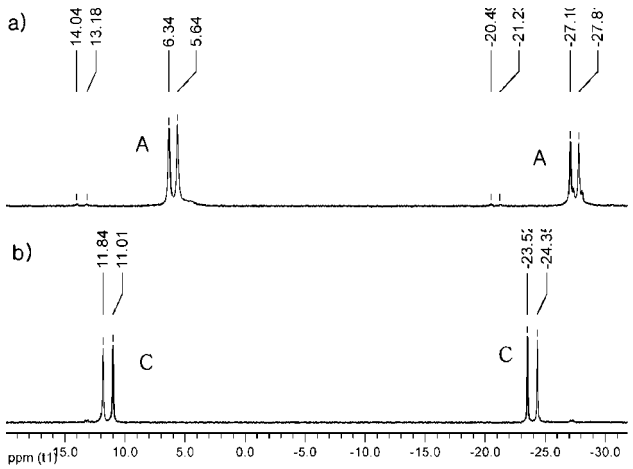

Figure 10. ^{31}P NMR spectra at −60 °C: (a) complex **1a** with 2 equiv of MeMgBr in toluene-d_8; (b) complex **1a** with 2 equiv of MeMgBr in THF-d_8.

supra). In toluene-d_8, the alkylcopper species, formed after the addition of MeMgBr to the complex **1a** with chemical shifts at 5.9 and −27.4 and J_{p-p} = 143 Hz, is assigned to complex **A** (Figure 10a).[34a] By contrast, the addition of MeMgBr to **1a** in THF-d_8 led to formation of a Cu complex with two doublets (11.0 ppm and −23.9 ppm). On the basis of the coupling constant J_{p-p} = 163 Hz, we assigned the species formed in THF as complex **C** (Figure 10b).[34b]

The formation of **A** in toluene and **C** in THF is in agreement with the experimental results, which show a high regio- and enantioselectivity in toluene and poor selectivity in THF (Table 2, entries 2, 5). These results again confirm the importance of species **A** in the catalytic cycle, to achieve high levels of regio- and enantioselectivity. Any reaction parameter that contributes to the formation of species **A** appears to provide highly efficient catalysis, while all the reaction parameters promoting the formation of **C** lead to lower efficiency and selectivity of the present catalytic system.

Based on the product distribution and level of enantioselectivity, a second parameter which may have an impact on the formation of either **A** or **C** could be the halide employed in the copper source and Grignard reagent (Table 3). ^{31}P NMR spectra of complexes **1a** (X = Br) (Figure 7a), **1b** (X = Cl) (Figure 11a), **1c** (X = I) (Figure 12a) show only slight differences in the ^{31}P chemical shifts and in the value of the P−P coupling constant which depends on the type of halogen.

Addition of 4 equiv of MeMgCl to **1b**, led exclusively to the formation of the complex **C**, with no indication for the formation of complex **A** (Figure 11b). This correlates well with the poor result obtained in the CA of MeMgCl to **5**, catalyzed by copper chloride complex **1b** (Table 3, entry 5). In contrast, when 10 equiv of MeMgBr were added to **1b**, only formation of species **A** was observed (Figure 11c), which is in good agreement with CA results (Table 3, entry 2).[35]

The situation for the copper iodide complex **1c** was quite different (Figure 12 a−c). In this case the addition of MeMgI

(32) However, related diphosphine copper complexes bridged by alkyne moieties have been reported, for instance, see: Janssen, M. D.; Kohler, K.; Herres, M.; Dedieu, A.; Smeets, W. J. J.; Spek, A. L.; Grove, D. M.; Lang, H.; van Koten, G. *J. Am. Chem. Soc.* **1996**, *118*, 4817−4829.

(33) Due to the ^{1}H NMR downfield shift of the Cu*Me* signal and overlap with several other peaks in the above-mentioned solvents, the following studies were monitored by ^{31}P NMR spectroscopy only.

(34) (a) We assigned the alkylcopper species observed in toluene to the complex **A** based on the value of the J_{p-p} coupling constant. (b) Slight difference in chemical shifts is due to changing the solvent from CH_2Cl_2 to THF.

(35) The formation of **A** in this case of **1b** can be explained by the exchange of chloride (or iodide in the case of **1c**) by a bromide in the copper complex, due to presence of an excess of MeMgBr.

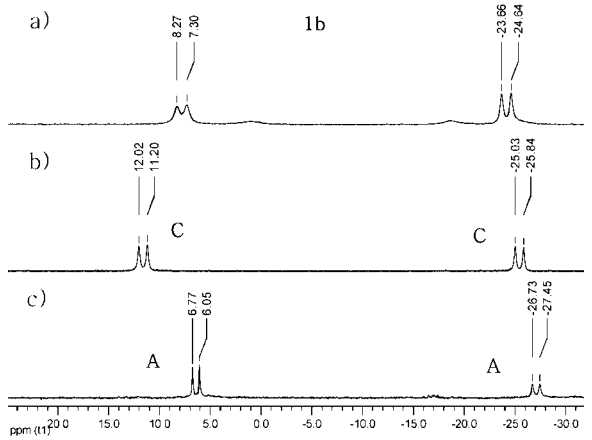

Figure 11. ^{31}P NMR spectra in CD_2Cl_2 at −60 °C: (a) CuCl complex **1b**. **(**b) **1b** with 4 equiv of MeMgCl. (c) **1b** with 10 equiv of MeMgBr.

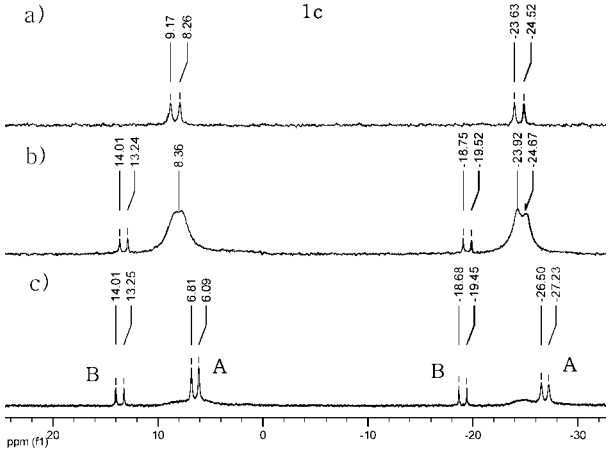

Figure 12. ^{31}P NMR spectra in CD_2Cl_2 at −60 °C: (a) CuI complex **1c**. **(**b) **1c** with 3 equiv of MeMgI. (c) **1c** with 10 equiv of MeMgBr.

caused signal broadening, corresponding to the initial complex **1c** and formation of a minor amount of **B** (vide supra and Figure 12b). A 3-fold increase in the concentration of MeMgI resulted in a slight increase in **B** and further broadening of the remaining resonances. Since no appreciable amount of species **A** or **C** is formed with MeMgI, the background reaction is most probably responsible for the low enantioselectivity observed in the catalytic reaction (Table 3, entries 6, 7). As for **1b**, when 10 equiv of MeMgBr were added to **1c**, only formation of species **A** was observed (Figure 12c), again in good agreement with the CA results.[35]

Finally, the sensitivity of the reaction to water and air was examined. A CD_2Cl_2 solution of **A**, being in contact with air, was transformed slowly to species **B**, as determined by ^{31}P NMR and ^{1}H NMR spectroscopy (Figure 13). The phosphorus resonances of **B** are shifted downfield to 13.62 ppm and −19.07 ppm relative to those of **A**. The ^{1}H NMR absorption of Cu*Me* appeared as a sharp singlet at −0.32 ppm, shifted upfield by 0.03 ppm compared to complex **A**. When 1 equiv of dioxane was added to **B**, no changes were observed by NMR spectroscopy.

Thus, we can consider that **B** is a side product accompanying the formation of the species **A** and **C**. Unfortunately, the precise structure of species **B** cannot be discerned from the data available.[36]

Alkene Geometry. The geometry of α,β-unsaturated carbonyl compounds is considered an important parameter to understand the mechanism of the stereocontrol in CAs. Therefore, the influence of the alkene (*cis*/*trans*) geometry on the enantioselective CA of EtMgBr to enones and enoates was examined, and a remarkable difference between ketones and esters was observed. (Scheme 7and Chart 2).

Surprisingly, in the present study, the CA of EtMgBr to both *trans*-**7** and *cis*-**7** enones, catalyzed by complex **1a**, afforded the product **12a** with the same absolute configuration and an equal level of enantioselectivity (Table 4, entries 1 and 2). In contrast, the CA of EtMgBr to both *trans*-**8** and *cis*-**8** enoates, catalyzed by **1a** led to the products **12b** with opposite configurations (entries 3, 4).

Analysis of the reaction mixture at different times led to the conclusion that an isomerization of the *cis*-enoates to the *trans*-isomer was occurring during the CA reaction of EtMgBr to enoates **9**−**11** (entries 6−13).

Lower enantioselectivities in the CA to the *cis*-enoates were achieved in these cases, and a *cis*−*trans* isomerization within the time scale of the reactions could be demonstrated also. The observation of this partial isomerization during the reaction provides an explanation for the low enantioselectivity obtained in the CA to *cis*-enoates **9**−**11**.[37a]

Furthermore, although no CA reaction occurred between MeMgBr and the less active *p*-OMe cinnamate *trans*-**11** or *cis*-**11**, isomerization was observed when the reaction was carried out with *cis*-**11**. Control experiments confirmed that the isomerization process is only initiated when both the chiral copper complex (**2a**) and the Grignard reagent are present in solution together with the *cis*-enoate.[37b]

This suggests that the activated copper complex **A** may interact directly, but reversibly, with the alkene moiety allowing the *cis*−*trans* isomerization of the double bond to occur, and therefore causing a decrease in the enantioselectivity of the reaction. When the *cis*−*trans* isomerization is much faster than the final irreversible step leading to the product, the formation of the adduct with the same absolute configuration either starting from the *cis*- or *trans*-unsaturated system may be expected. Indeed, this appears to be the case for the enones *trans*-**7** and *cis*-**7**.

Kinetic Analysis. The intermediate species derived from the substrate (enone or enoate) and complex **A**, which is postulated to be the key complex involved in the catalytic cycle, could not be detected directly due to their transient existence and hence, low concentration. A kinetic analysis of the CA reaction could provide insight into the reaction mechanism; however, several difficulties are associated with the model reaction (the addition of MeMgBr to octenone) discussed thus far with regard to kinetic studies. In particular, the very high reaction rate even at −78 °C, an incomplete regioselectivity (∼85%), and the

(36) Interestingly, 90% ee was obtained when the stoichiometric reaction with the **5** was performed with species **B**. Nevertheless, the participation of species **B** in the catalytic cycle is unlikely, since under reaction conditions and accordingly, in the presence of large excess of Grignard reagent and **5**, fast formation and consumption of species **A** will prevent any role of species **B**.

(37) (a) The higher enantioselectivity observed in the CA of EtMgBr to *cis*-**8** (Table 4, entry 3) is attributed to the faster conjugate addition to β-alkyl- compared to β-aryl α,β-unsubstituted esters (Table 4, entries 7, 10, 13). (b) In the absence of Grignard reagent, or Cu complex **(1a** or **2a)**, or in the presence of Grignard reagent with $CuBr{\cdot}SMe_2$ instead of the chiral complex no isomerization was observed.

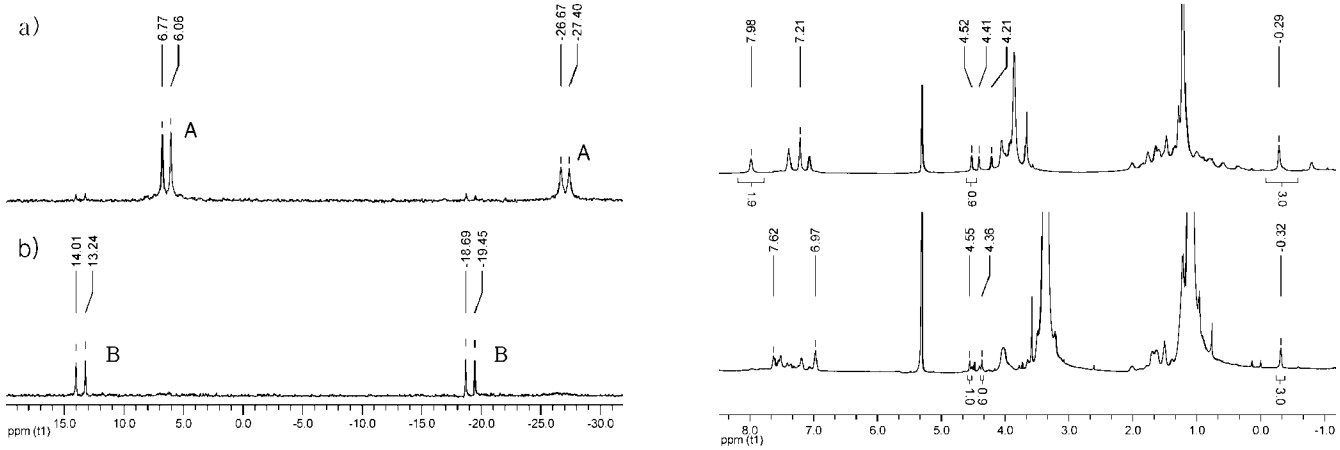

Figure 13. ^{31}P NMR (left) and ^{1}H NMR (right) spectra in CD_2Cl_2 at −60 °C: (a) species **A** formed from complex **1a** with 4 equiv of MeMgBr. (b) Species **B** formed from **A** under influence of air.

Scheme 7. Enantioselective CA of EtMgBr to *cis*- and *trans*-α,β-unsaturated Compounds

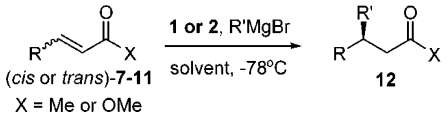

Chart 2

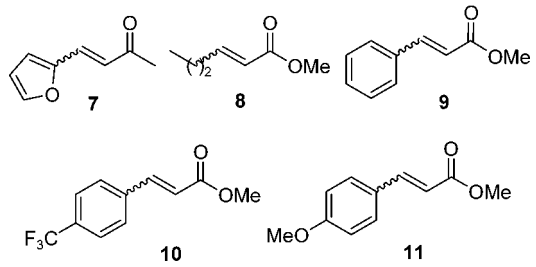

Table 4. CA of EtMgBr and *cis*−*trans* Isomerization of Substrates[a]

entry	substrate	catalyst[b]	conv. **12** [%][c]	*cis:trans* [%][d]	ee [%][c]
1	*trans*-**7**	**1a**	100 (**12a**)	−	95 (+)
2	*cis*-**7**	**1a**	100 (**12a**)	−	95 (+)
3	*trans*-**8**	**1a**	100 (**12b**)	−	90 (*R*)
4	*cis*-**8**	**1a**	100 (**12b**)	−	90 (*S*)
5[e]	*cis*-**8**	**1a**	50 (**12b**)	99:1	90 (*S*)
6	*trans*-**9**	**2a**	100 (**12c**)	−	98 (*S*)
7	*cis*-**9**	**2a**	100 (**12c**)	−	53 (*R*)
8[e]	*cis*-**9**	**2a**	10 (**12c**)	94:6	59 (*R*)
9	*trans*-**10**	**2a**	100 (**12d**)	−	96 (+)
10	*cis*-**10**	**2a**	100 (**12d**)	−	63 (−)
11[e]	*cis*-**10**	**2a**	85 (**12d**)	86:14	67 (−)
12[f]	*trans*-**11**	**2a**	70 (**12e**)	−	90 (−)
13[e,f]	*cis*-**11**	**2a**	77 (**12e**)	1:99	40 (+)

[a] Reaction conditions: ^{t}BuOMe as a solvent, EtMgBr 1.5 equiv, −78 °C. [b] 5 mol % (*R*,*S*)-**1a** or (*S*,*R*)-**2a**. [c] Determined by GC. [d] *cis:trans* ratio of the recovered starting material. [e] Reaction was stopped after ∼10−80% conversion. [f] 5 mol % (*R*,*S*)-**2a**.

background reaction prevents the collection of reliable data. On the other hand, CA of Grignard reagent to enoates proceeds with high enantioselectivity similar to that of enones and shows comparable dependence on the reaction solvent and copper halide.[7c] Moreover, this reaction offers considerable advantages for kinetic analysis due to its significantly slower rate, higher regioselectivity (99%), and the absence of any side products or background reaction at low temperature. The very low reactivity

Scheme 8. CA of EtMgBr to Methyl Crotonate **13**, Catalyzed by Cu-Bromide Complex **1a**

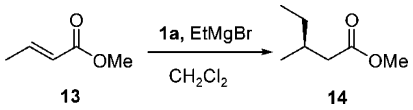

between MeMgBr and enoates prompted us to use the more reactive EtMgBr for these studies. Thus, the addition of EtMgBr to methyl crotonate **13**, catalyzed by the Cu-complex **1a** in CH_2Cl_2 at −87 °C, was chosen as model reaction for the kinetic study (Scheme 8).

The reaction rates were measured at varying concentrations of substrate, Grignard reagent, and catalyst. The effects of the initial concentrations of **13** and EtMgBr were examined within a range of 0.09 to 0.36 M (see Supporting Information).[38a] By measuring the reaction rate at different concentrations of EtMgBr (up to 80% conversion) an enhancement of the reaction rate was found at increased concentration of the Grignard reagent. The kinetic analysis for the substrate **13** were impeded by a side reaction,[38b] which occurred at increased substrate concentrations (more than 2 equiv of **13**). Nevertheless, as for EtMgBr, an increase in reaction rate with increasing substrate concentration was observed (1−2 equiv). The dependence of the reaction rate on [EtMgBr] (vide supra) and [**13**] suggests that both reactants are involved in the rate-limiting step.

The rate constant calculated at different initial concentrations of the precatalyst allowed determination of the order of the reaction with respect to the catalyst (1.17 for complex **1a**), by plotting the (ln *k*) against ln[C_o] of catalyst **1a** (Figure 14).[38c]

From the spectroscopic and electrochemical analysis of the copper complexes (vide supra) it is clear that complex **1a** in CH_2Cl_2 forms a dimeric structure and that the association constant is very high. However, complex **1a** is only a precatalyst**,** and after addition of Grignard reagents, formation of the catalytically active species (i.e. **A**) occurs (vide supra). If the catalyst is a dinuclear species, then the order of the reaction

(38) (a) Graphical representation of the experimental kinetic data is presented in the Supporting Information. Due to the formation of a side product and the presence of a suspension at the conditions required for a pseudo-first-order kinetic analysis this approach could not be applied to this reaction to determine the reaction order in both Grignard reagent and substrate. (b) The side product detected corresponds to the Michael addition of the generated enolate to another molecule of substrate **13**. (c) Best-fit lines were obtained by the least-squares method.

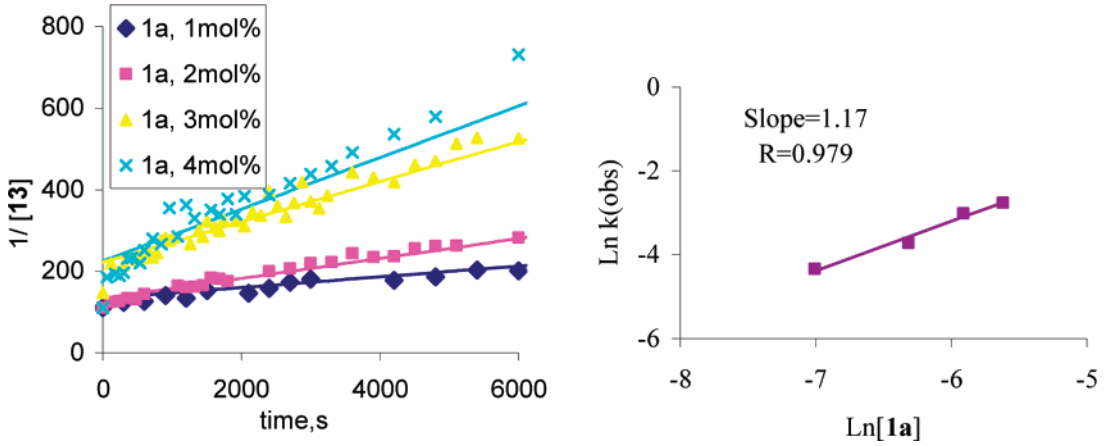

Figure 14. Rate measurements for the CA of EtMgBr to **13**, catalyzed by **1a** in CH_2Cl_2 at −87 °C: (a) kinetic data obtained for different catalyst concentrations, (b) reaction order with respect to **1a**.

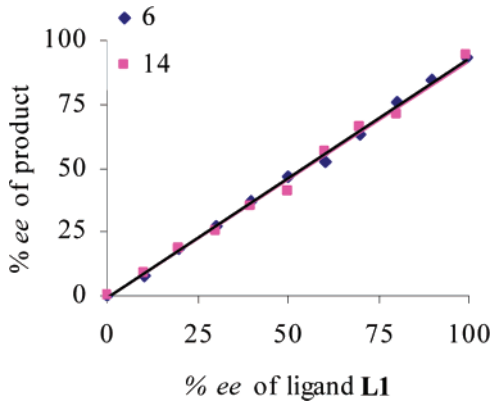

Figure 15. Linear relationship between ee of ligand **L1** and ee of the products **6** (◆) and **14** (solid red square) obtained by the addition of MeMgBr and EtMgBr to octenone **5** and methyl crotonate **13**, respectively, catalyzed by **1a** in CH_2Cl_2 at −78 °C.

Scheme 9. CA of EtMgBr to Methyl Cinnamate

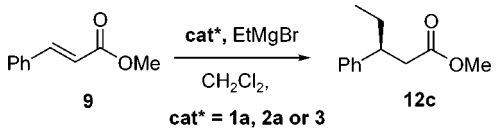

with respect to the precatalyst will be between one and two with the exact value depending upon the equilibrium constant between the mononuclear and the dinuclear species. However, if the catalyst is a mononuclear copper species (as attributed for species **A** above), then the order of the reaction with respect to the precatalyst should be closer to one. The latter is consistent with the experimental results (1.17) and indicates that the active form of the catalyst is a mononuclear complex. This assignment is supported by the linear relationship between the product and the catalyst enantiomeric purity (Figure 15).

Additional evidence for the mononuclearity of the catalytically active species was obtained by the comparison of the catalytic activity of heterocomplex **3** with that of homocomplexes **1a** and **2a**, in the CA of EtMgBr to methyl cinnamate **9** (Scheme 9).

Table 5. CA of EtMgBr to **9** in CH_2Cl_2, Catalyzed by Copper Bromide Complexes **1a**, **2a**, and **3**[a]

entry	catalyst [mol %]	conv. [%][b]	ee [%][c] (*R*/*S*)
1	(*R*,*S*)-**1a** [2.5]	4	72 (S)
2	(*S*,*R*)-**2a** [2.5]	69	98 (R)
3	**3** [2.5]	32	95 (R)
4	**3** [5.0]	65	96 (R)

[a] Reaction conditions: concentration of **9** 0.35 M, EtMgBr 1.5 equiv, −78 °C, 3 h. [b] Conversion (GC) after 3 h. [c] Determined by GC on chiral dex-CB column.

As demonstrated in a previous report,[7c] complex **1a** is a very poor catalyst in the CA of Grignard reagents to α,β-unsaturated aromatic esters, while complex **2a** (prepared from **L2** and CuBr) is very efficient in this reaction. Indeed, complex (*R*,*S*)-**1a** shows very poor catalysis in the present reaction leading to the product **12c** with only 4% conversion and 72% ee (Scheme 9, Table 5, entries 1). In contrast, complex (*S*,*R*)-**2a** afforded, in the same reaction time, the desired product with a good conversion of 69% and an excellent ee (98%) (Table 5, entries 1, 2).

If a mononuclear complex derived from complex **3** (Scheme 10) is the active catalyst, then it would be expected that the outcome of the reaction would be almost identical to that obtained with the most efficient catalyst **2a**. That this is indeed the case is supported by the experimental results (Table 5, entries 3 and 4).

The rate and enantioselectivity observed in the reaction catalyzed by **3** were nearly identical to those obtained with (*S*,*R*)-**2a** (entries 3, 4). This result suggests that the dimeric copper bromide complex **3** is dissociated upon addition of the Grignard reagent (Scheme 10) and a catalytically active mononuclear complex derived from **2a** is responsible for the stereoselective reaction.

Finally, the activation parameters were determined for the CA of EtMgBr to **13** (Scheme 8) from kinetic measurements

Scheme 10. Dissociation of the Complex **3** upon Addition of Grignard Reagent

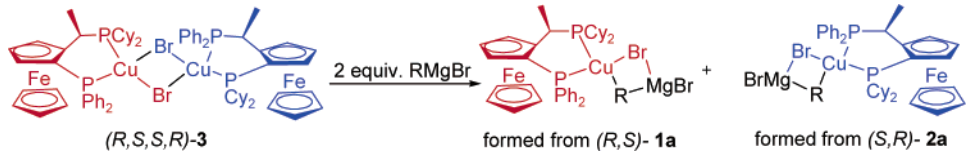

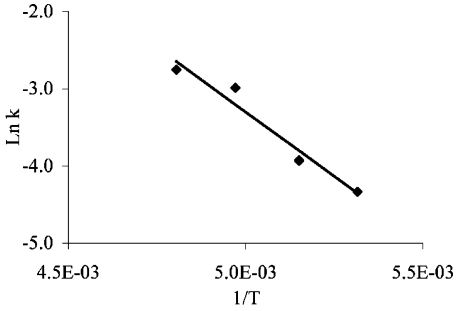

Figure 16. Arrhenius plot for the CA of EtMgBr to **13**, catalyzed by **1a** in CH_2Cl_2.

Table 6. Thermodynamic Parameters for CA of EtMgBr to Methyl Crotonate **13** Catalyzed by **1a**

thermodynamic parameters	values
E_a (kJ·mol^{-1})	28
$\Delta H^{\ddagger}$ (kJ·mol^{-1})	26
$\Delta S^{\ddagger}$ (J·K^{-1}·mol^{-1})	−138
$\Delta G°$(20 °C) (kJ·mol^{-1})	66
k^0 (20 °C) (L·mol^{-1}·s^{-1})	4.8
$t_{1/2}$ (20 °C) (s)	23.3

Scheme 11. Proposed Catalytic Cycle for the CA Addition of Grignard Reagents to α,β-Unsaturated Carbonyl Compounds

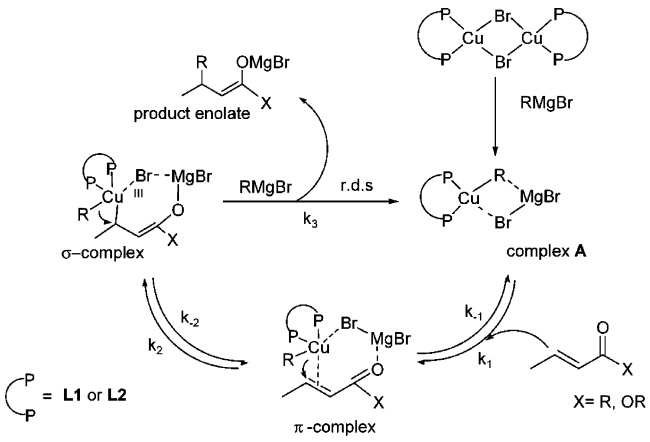

carried out at −65, −70, −80, −85 °C. The Arrhenius plot of rate constants vs reciprocal temperature (T^{-1}) is presented in Figure 16.

An Eyring analysis of the kinetic data for the reaction provides the activation parameters which are presented in Table 6. The energy of activation, $E_a = 27.7$ (kJ·mol^{-1}), for the present reaction can be compared with the value of $E_a = 76$ (kJ·mol^{-1}) obtained by Krause for the noncatalytic 1,4-organocuprate addition.[9b,39]

Mechanistic Discussion of the Enantioselective CA of Grignard Reagents to α,β-Unsaturated Carbonyl Compounds. A reaction pathway, which is consistent with the experimental results and kinetic and spectroscopic data collected in this study, is proposed in Scheme 11. The pathway of the CA reaction involves formation of an intermediate species via π-complexation followed by formation of a magnesium enolate through a Cu(III) intermediate. The first step in the catalytic cycle is initiated by formation of the catalytically active complex **A**. The monomeric complex **A** is formed from dimeric precatalyst **1a** via transmetalation with Grignard reagent (Scheme 11). Most probably, complex **A** functions in a similar manner as organocuprates with the additional advantage that it bears a chiral diphosphine ligand which accelerates the CA process and stabilizes the reaction intermediates, thus overcoming background 1,4- and 1,2-additions.

The first intermediate in the proposed cycle is the π-complex in which **A** forms, reversibly, a complex with the double bond of the enone (enoate) through copper with an additional interaction of Mg^{2+} with the oxygen atom of the carbonyl moiety (Scheme 11). The importance of Mg^{2+} is reflected in the inhibitory effects of solvent (THF), additive (dioxane), and halide (absence of bromide) on the conversion and stereo-/regioselectivity of the reaction. These inhibitory effects are due to the formation of species **C** (Scheme 6), which is triggered by removal of Mg^{2+} from the system.

The results indicate that Mg^{2+} not only activates the enone (enoate) via coordination with oxygen (Lewis acid effect), but also associates to the Cu-complex through the bridging halogen. The importance of bromide in the halide bridge is evident from the observations that its presence in either the initial Cu-complex or Grignard reagent is essential to form species **A**. The origin of this effect is unclear; however, the size and electronegativity of bromide may be critical in achieving a balance between stabilization of the π- and σ-complexes, which are intermediates in the reaction. Furthermore we have shown that the CuI and CuCl bonds in the complexes **1b**, **1c** are sufficiently labile to be exchanged by the bromide present in the Grignard reagent. The formation of a π-complex is possibly followed by intramolecular rearrangement to a Cu(III)-intermediate where copper forms a σ-bond with the β-carbon of the enone (enoate). This σ-complex is in fast equilibrium with the π-complex, and the equilibrium constant between both complexes depends on the stability of the Cu(III)-intermediate. Theoretical calculations reported by Nakamura and co-workers[11d] for organocuprate CA to enones indicate that this type of Cu(III) intermediate should be very unstable. These authors propose that thermodynamic stabilization of the Cu/substrate species and kinetic lability toward reductive elimination, are the most important factors to accelerate the rate of C−C bond formation. Thermodynamic stabilization can be achieved by using soft donor ligands, while kinetic lability will depend mostly on geometry of the species formed. In the present system this is realized through a combination of Grignard reagent and a diphosphine ligand, which provides donor ligands and the necessary geometry in the σ-complex to afford excellent regio- and stereocontrol.

The proposed catalytic cycle can rationalize the observed *cis*−*trans* isomerization of enoates. This isomerization provides strong evidence for the presence of a fast equilibrium between the π-complex and the Cu(III) species (σ-complex), which is followed by the rate-limiting, reductive elimination step (Scheme 11). The observation that *cis*−*trans* isomerization occurs even in the case of the reaction between MeMgBr and the unsaturated enoate *cis*-**11**, which does not afford any detectable amounts of the product, is in agreement with the mechanism proposed. Cuprate-induced isomerization of a *cis*-enone to a *trans*-enone was reported previously by House[40] and was explained via

(39) The lower value of the E_a obtained for the present reaction as opposed to the system studied by Krause (ref 9b) might be due to the diphosphine moiety present in the structure of the catalyst, which significantly lowers the activation barrier of the transition state in the rate-limiting step.

(40) (a) House, H. O. *Acc. Chem. Res.* **1976**, *9*, 59. (b) House, H. O.; Weeks, P. D. *J. Am. Chem. Soc*, **1975**, *97*, 2770−2778.

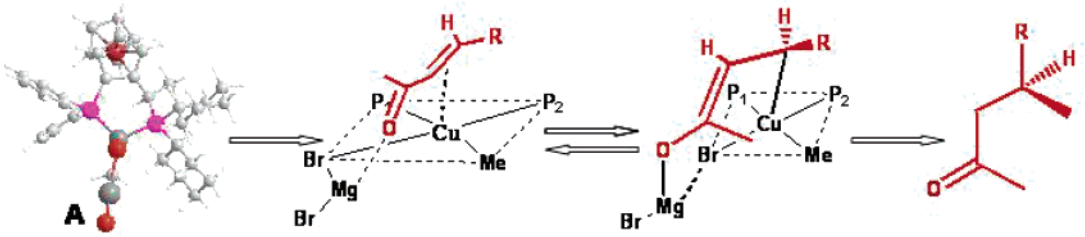

Figure 17. Working model for the enantioselective CA of Grignard reagents (P_1-diphenyl-substituted phosphine, P_2-dicyclohexyl-substituted phosphine).

formation of a radical anion involving electron transfer from the cuprate to the enone. Similar observations were subsequently reported by Corey and co-workers[9k] for CA of organocuprates. These authors concluded that the CA reaction of cuprates proceeds via a reversible d,π-complex and a Cu(III) adduct and that the initial electron-transfer step from cuprate to enone is not obligatory. The latter proposition is in good agreement with the properties observed for this catalytic system.

Additional support for the complexation of alkylcopper species **A** with the alkene moiety of the substrate as well as the rate-limiting alkyl-transfer step arises from the fact that any additional substitution at the α- or β-carbons of the substrate prevents formation of the 1,4-product. The presence of substituents at these positions might impede the coordination of the bulky diphosphine copper complex with the double bond, and consequently the 1,2-addition becomes the most favorable reaction for the active enone substrates, whereas no reaction with less active enoates was observed.

Finally, the proposed catalytic cycle correlates well with the results of the kinetic studies. The dependence of the reaction rate on the substrate and Grignard reagent indicates that both reactants are involved in the rate-limiting step preceded by fast equilibria between reactants and reaction intermediates. Furthermore, the rate of the decomposition of the Cu(III) species to the π-complex must be faster than the rate of its formation ($k_{-2} \gg k_2$, Scheme 11). This instability of the Cu(III) intermediate will prevent its accumulation in the rate-limiting step. The dependence of the reaction rate on the Grignard reagents suggests that it acts to displace the product from the Cu(III) intermediate and reform the catalytically active complex **A** directly (Scheme 11). Consequently, increasing the concentration of both reactants will enhance the reaction rate.

Optimized semiempirical [PM3(tm)] calculations indicate that complex **A** adopts a distorted tetrahedral structure with the positioning of the Grignard reagent at the bottom face of the complex (Figure 17).[41]

In the working model that we proposed for the enantioselective 1,4-addition of Grignard reagents it can be envisioned that the enone approaches the alkylcopper complex **A** from the least hindered side and binds to the top apical position. This forces the complex to adopt a square pyramidal geometry, which is stabilized via π-complexation of the alkene moiety to the copper and, importantly, through the interactions between Mg and the carbonyl moiety of the skewed enone.[42−44] It should be noted that [reversible] formation of a copper−alkene complex is well precedented, and this is supported by the ability of the catalytic system to effect *cis*−*trans* isomerization (vide supra). In the next step the formation of a transition structure with the chairlike seven-membered ring conformation is proposed, where copper forms a σ-bond approaching from the bottom side of the β-carbon. Most probably the absolute configuration is already fixed in the Cu(III) intermediate, and to avoid steric interactions with the dicyclohexyl moieties at the nearby phosphorus, the final transfer of methyl group occurs as shown in Figure 17. Although this model predicts the correct sense of asymmetric induction, it is nevertheless a hypothetical model and should be considered with care as it is difficult to rule out other possibilities due to the complex nature of the present system. Further mechanistic studies and DFT or ab initio calculations will be performed soon to shed light on to the factors that determine the origin of the enantioselectivity.

Conclusions

The combination of spectroscopic studies to identify the catalytically active species, kinetic analysis, and variation of reaction parameters provides a mechanistic scheme for the enantioselective CA of Grignard reagents to α,β-unsaturated carbonyl compounds, catalyzed by ferrocenyl diphosphine complexes. We have identified several parameters (the influence of solvent, halide, and additives) that affect the selectivity and rate of the CA reaction and define the structures of catalytically active species formed via transmetalation of a chiral copper complex by a Grignard reagent. Furthermore, the formation and structure of the active species was found to be highly dependent on the Schlenk equilibrium, which also depends on the solvent, nature of the halide, and the presence of additives. Moreover, we have demonstrated and rationalized that the presence of Mg^{2+} and Br^- ions is a necessary condition to achieve high selectivity and efficiency in the present system. Our results demonstrate furthermore that the rate of the reaction is dependent on all the reacting components, and is first order in catalyst.

The data presented supports a model in which the rate-limiting step is a reductive elimination, which is preceded by a fast

(41) Calculations were carried out using *HyperChem*, release 6.0 for Windows, Molecular Modelling system; Hypercube, Inc., 2000. Preliminary semiempirical [PM3(tm)] calculations were performed in the Cu complex **1a′**, to show the viability of this theoretical level to describe these Cu−halide complexes. The minimization of the complex at this level of theory provided a structure which retained the trigonal planar structure and which is qualitatively in accordance with the original structure obtained by X-ray analysis.

(42) In this construct, the BrMgBr occupied the less hindered side next to diphenylphosphine moieties (P_1), while the smaller methyl group shifts to the more bulky dicyclohexylphosphine (P_2) moieties.

(43) The resulting structure could also be obtained and its energy minimized; however, the distance between the Cu and the double bond turned out to be much higher than that required to establish a π interaction, suggesting that the semiempirical level is not suitable to model these interactions between Cu and double bonds.

(44) We propose the π-complex formation from the *S-trans* conformer of the enone, and although the *S-cis* conformer cannot be excluded, appropriate binding of Mg and Cu simultaneously with the enone in the *S-cis* conformation is less favorable. For studies on *S-trans/S-cis* conformational preferences of α,β-unsaturated carbonyl compounds, see: (a) Garcia, J. I.; Mayoral, J. A.; Salvatella, L.; Assfeld, X.; Ruiz-Lopez, M. F. *J. Mol. Struct.* **1996**, *362*, 187−197. (b) Shida, N.; Kabuto, C.; Niva, T.; Ebata, T.; Yamamoto, Y. *J. Org. Chem.* **1994**, *59*, 4068−4075.

equilibrium involving a Cu(I)-π-complex/Cu(III)-σ complex adduct. The influence of olefin geometry on the reaction selectivity and the observation of *cis*−*trans* isomerization for enoates along the reaction pathway support this mechanistic model. Although these investigations clarify a significant portion of the mechanistic pathway, there are still important aspects that remain to be elucidated, most importantly, a detailed picture of the mechanism of stereoselection in this reaction.

Acknowledgment. Financial support from the Dutch Ministry of Economic Affairs (EET scheme; Grant Nos.: EETK-97107 and 99104) and the European Community's 6th Framework Program (Marie Curie IntraEuropean Fellowship to F.L.) is acknowledged. A.C. was supported by a predoctoral grant from the Departamento de Educación, Universidades e Investigación del Gobierno Vasco. D.P. thanks the European Community (IHP Program) for the award of a Marie Curie Fellowship (Contract HPMF-CT-2002-01612). We are grateful to Dr. H.-U. Blaser (Solvias, Basel) for a generous gift of Josiphos ligands, and we thank T. D. Tiemersma-Wegman for GC and HPLC support.

Supporting Information Available: Experimental procedures and spectroscopic data, X-ray data, solvent and halide dependence of CA of EtMgX to enoates and kinetic data. This material is available free of charge via the Internet at http://pubs.acs.org

JA0585634